NOTICE

THIS DOCUMENT HAS BEEN REPRODUCED FROM MICROFICHE. ALTHOUGH IT IS RECOGNIZED THAT CERTAIN PORTIONS ARE ILLEGIBLE, IT IS BEING RELEASED IN THE INTEREST OF MAKING AVAILABLE AS MUCH INFORMATION AS POSSIBLE

LABORATORY SIMULATION OF IRRADIATION-INDUCED DIELECTRIC BREAKDOWN IN SPACECRAFT CHARGING

FINAL REPORT
NASA Research Grant No. NSG-3145
April 1, 1977 to November 30, 1979

Submitted by

Edward J. Yadlowsky
Russell J. Churchill
Robert C. Hazelton

RESEARCH AND DEVELOPMENT CENTER
INLAND MOTOR DIVISIONS
KOLLMORGEN CORPORATION
501 First Street
RADFORD, VIRGINIA 24141

SUBCONTRACTORS TO:

COLORADO STATE UNIVERSITY
FORT COLLINS, COLORADO 80523

February 13, 1980

INTRODUCTION

There is a rapidly developing body of literature[1] in which the problems encountered by spacecraft at synchronous orbits have been delineated. It has now been indicated[2] that the significant electrical currents which flow during a discharge on a satellite give rise to electromagnetic fields manifested by electrical interference in communications, by commands affecting control, and by exterior and interior material damage to insulators and solid state components. Because of this it is of special interest to system designers to know of the temporal properties of the electrical discharges, the magnitudes of the involved currents, and the physical extent of the discharges over the spacecraft surface. With such information the spacecraft designer is armed with a powerful tool by which he is able to alleviate the effect of electrical discharges by careful selection of material size and by the strategic location of conductive electrodes through which electrical discharges may be channeled at threshold potentials much less than those which define serious damage and other deleterious effects. Toward this goal researchers have sought methods of delineating the electrical discharge properties in a quantitative manner[3-7] and have developed models for describing the discharge processes.[8-10]

As part of this research effort, Colorado State University, under a NASA Grant (NSG-3145), had undertaken a program to investigate the discharging of dielectric samples irradiated

by a beam of mono-energetic electrons (0-34 keV). The principal objective of this program is the identification of a model, or models, which describe the discharge phenomena which occurs on the irradiated dielectric targets. Specific goals in this program include:

A) Study of the electrical discharge characteristics of irradiated dielectric samples.

B) Determination of the origin and destination of surface-emitted particles.

C) Determination of electrical discharge paths along dielectric surfaces and within the dielectric material.

D) Evaluation of the charge and energy balance in the system as an aid in the development of models of the discharge phenomena.

The discharge paths are ascertained from visual observations and photographs of the self-luminous discharge together with material damage studies using optical and scanning electron microscopy. Faraday cups and retarding potential analyzers are used to measure the angular distribution and the energy distribution of the emitted particles and a charge collector determines the total charge in the flux of emitted particles for charge balance considerations. Additional characteristics of the discharge have been obtained from measurements of the beam voltage required to initiate a discharge, light emission, transient return currents and surface voltage profiles before and after discharges.

The results indicate that the dielectric samples are discharged by lateral currents flowing on or beneath the sample surface. Material properties play an important role in determining threshold voltages and discharge paths with Teflon exhibiting a pronounced anisotropy which could substantially limit the surface area that can be discharged during a given event. The emitted particle measurements indicate that plasma effects can be important in establishing conducting channels within the dielectric. The emitted particles act as a probe to provide information about the temporal evolution of the emitting site potential. Further, the measurements indicate that dielectrics can be discharged by two different physical mechanisms and that the duration of the return current pulse is a convenient signature to distinguish between these processes.

This program was transferred from Colorado State University to the Research and Development Center of Inland Motor Divisions, Kollmorgen Corporation in June of 1979 where the work was completed under a subcontract from Colorado State University. The final report is divided into an Experimental System section followed by a section describing the Measurement Techniques and Results and a Discussion of Results section.

EXPERIMENTAL SYSTEM

The breakdown process and subsequent discharge of a
dielectric surface have been studied by electron beam irradi-
ation of a Teflon target located in a vacuum chamber (Fig. 1).
The chamber consists of a 30cm diameter cylindrical glass tube
about 1 meter in length. Four cylindrical ports 15cm in
diameter located at the central section of the tube provide
outlets for vacuum ports, introduction of electrical and photo-
graphic measurement systems and the installation of target
assemblies. The electron gun is located at one end of the 30cm
diameter cylinder and generates an axial electron beam directed
toward a centrally-located target area. Base pressures of
10^{-7} Torr are possible using a 10cm diameter oil diffusion pump
system.

The dielectric targets are bombarded with a divergent
mono-energetic electron beam having an acceleration potential
from 0 to 34kV and a beam current density at the target location
of $0-5nA/cm^2$. Uniformity of the electron beam over the target
area is about 25% for a 10cm diameter target located 50cm from
the electron gun.

During the course of this project two distinct target
assemblies have been used for various measurement techniques.
In the first case (Fig. 2), the target assembly was mounted at
an angle of 40° to the incident electron beam. This configu-
ration allowed the measurement of particles emitted normally
from the dielectric surface without interfering with the
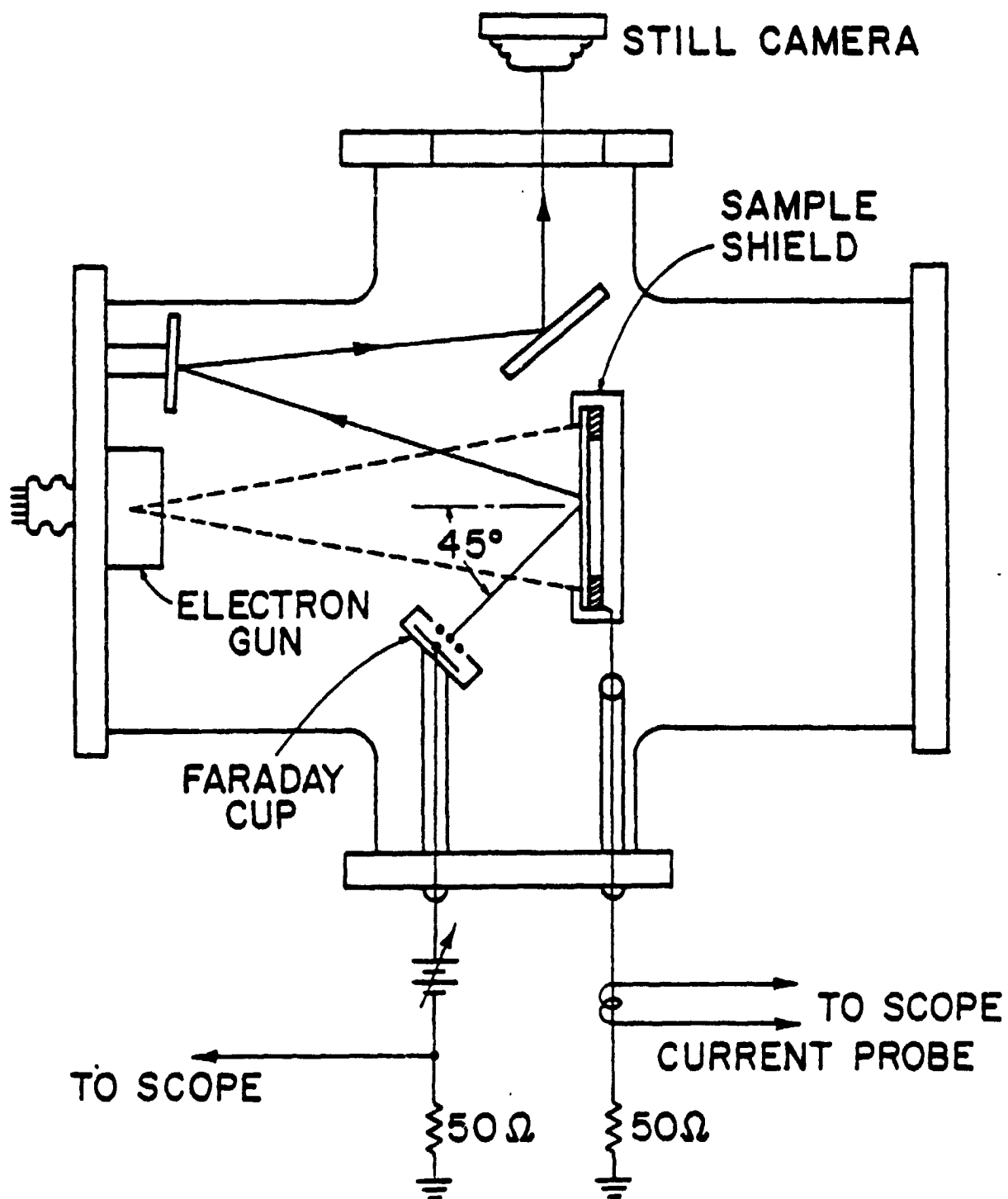incident beam. The sample was attached to an annular ring

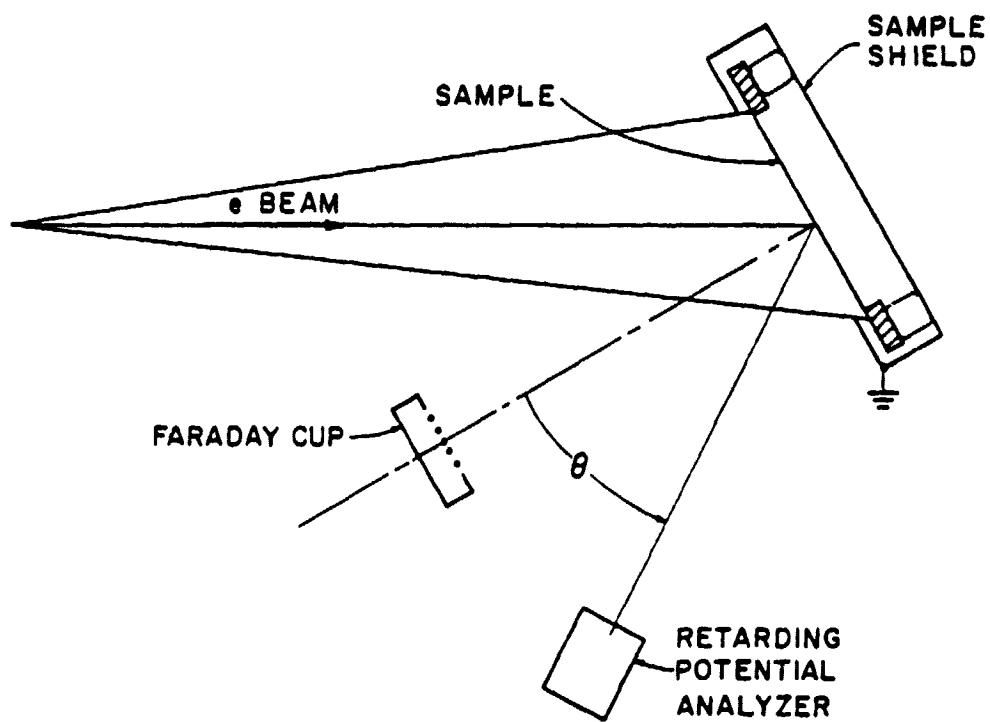Figure 1. Spacecraft charging simulator and measurement system.

Figure 2. Angular distribution measurement system
(relative orientation of dielectric sample,
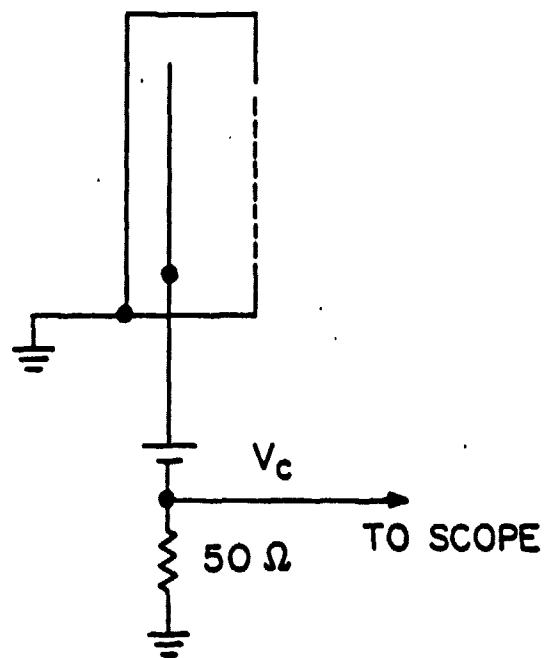electron beam and charged particle detectors).

(10cm diameter) by means of a conductive silver paint. The entire sample holder is placed within, but electrically insulated from, an enclosure containing an aperture through which the sample is irradiated. In this manner the sample edges are shielded from direct irradiation by the electron beam, thus facilitating breakdown studies not dominated by edge effects. In addition, edges can be selectively exposed for measurements of edge breakdown phenomena. The aperture can be varied during operation from 2.5cm to 8cm in diameter by externally controlling the opening of an adjustable iris mounted on the sample enclosure to facilitate the study of discharge properties which depend on the surface area irradiated. In this configuration the front surface is visible for inspection and photographic measurements.

Charged particle measurements are made using a biased Faraday cup and a retarding potential analyzer (RPA), both of which are illustrated in Figure 3. The Faraday cup consists of a shielded collector which can be biased to collect either positive or negative particles through a grid aperture of 2.5cm. The output current of the collector is shunted to ground through a 50 ohm load and the resulting voltage is measured with a Tektronix 556 oscilloscope.

The retarding potential analyzer used for the measurement of emitted particles consists of a particle collector plate and two independently biasable grids enclosed in a grounded shield having an input aperture of 1.2cm. For the measurement of positive particles the collector is biased at -9V to capture

(a)

V_c

TO SCOPE

50 Ω

(b)

V_c

V_{G2}
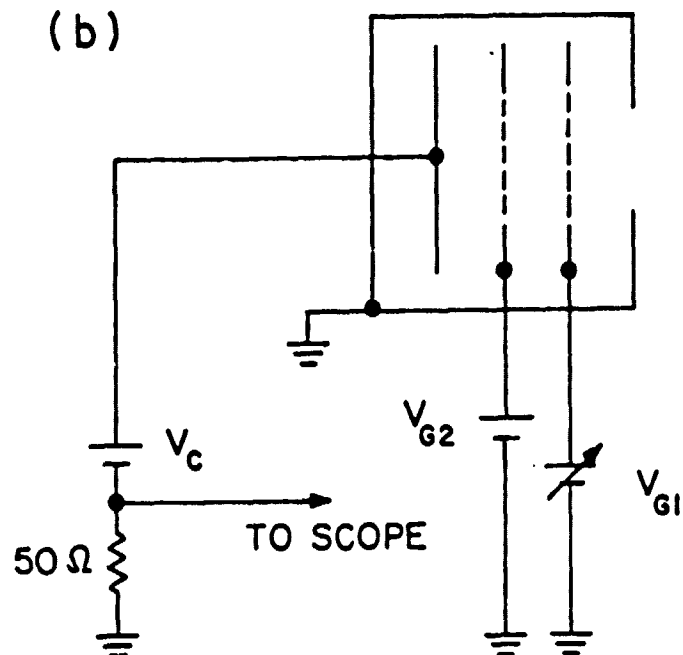
V_{G1}

50 Ω

TO SCOPE

Figure 3.   Charged particle detectors:
            (a) Faraday cup
            (b) Retarding potential analyzer.

the positive particles which pass through the grids. Grid G2, the suppressor grid, is biased at -800V to prevent secondary electron emission from the collector surface which could be erroneously interpreted as positive particles. The first grid is then biased positively to define a threshold energy for the incoming particles. By varying the bias on the first grid the energy spectrum of the incoming ions can be measured.

The output of the collector is measured in a manner identical to that used with the Faraday cup. A temporally-resolved particle flux is thereby derived and particle transit times and total particle emissions are determined. Similar measurements are made for negative particles with the collector biased to +9V, the second grid grounded, and the first grid biased negatively. In all cases the amplitudes of the incident particle fluxes are derived by multiplying the measured signal by the weighting factor of 1.8 to account for grid attenuation. The distribution of particle energies is obtained by graphical differentiation of the measured dependence of collector current on retarding grid voltage.

For the angular measurements presented herein, the probes were positioned as shown in Figure 2. The sample is tilted at an angle $\sim 40°$ to the beam axis to allow observation of normally emitted particles free from detector interference with the beam. The Faraday cup is set at a fixed angle of $40°$ below the horizontal plane, 9.5cm from the sample surface. The RPA is located about 15cm from the sample center and is free to pivot some $70°$ about the sample center line. The

entrance aperture of the RPA subtends an angle of 3° with respect to a point on the target surface.

A high energy retarding potential analyzer (HERPA) was designed to provide a retarding potential of up to 11 kV. The HERPA is positioned 9.2cm from the sample surface and has an aperture of 5.6cm. Measurements are made in a fashion identical to that of the RPA.

The electron beam voltage required to initiate a breakdown is determined by irradiating the sample to equilibrium conditions with successively increased electron beam voltages (in 2 kV increments) until a breakdown occurs. Since direct measurements of the target surface potential were not available at the time breakdown thresholds were measured, the equilibrium electron beam voltage has been taken as a measure of the surface voltage prior to the initiation of an electrical breakdown as previously suggested by Berkopec et al.[5]

The transient current that flows to the silver-backing on the sample during a discharge event is measured by a Tektronix CT-1 current probe clipped around the lead connecting the silver-backing to ground potential.

A system of mirrors and viewing ports permits time-integrated photographs of the self-luminous electrical discharge to be taken. The resultant photographs of the discharge path along the sample surface and of the central site of the discharge are correlated with scanning electron microscope studies of material damage.

A new experimental configuration was designed and con-
structed to accommodate the installation of a surface voltage
probe (TREK Model 340HV) and to facilitate the measurement of
the total emitted charge for charge balance studies. The basic
features of the previous system have been retained. The sample
is mounted on a solid aluminum disc, in this case, using a
conductive silver paint, and the return current to ground is
again measured with a Tektronic CT-1 probe. The sample edges
are shielded by a variable diameter (4-13cm) iris allowing
selective studies of edge breakdowns or puncture breakdowns.

A significant new feature in the system is an X-Y scanning
probe mount for two dimensional surface potential profile and
electron beam profile measurements. The X and Y axes are
equipped with counters to provide position information as the
probe is scanned. The Y axis is also equipped with a potenti-
ometer and d.c. power source to provide a voltage proportional
to position for automatic recording of surface potential scans.
In operation the surface voltage probe is 0.2cm from the sample
surface providing surface resolution of this magnitude.

The other new feature in the system is a detector to
measure the total current emitted during a discharge event.
The detector consists of a cylindrical enclosure 28cm diameter
x 35cm long with a 6cm diameter aperture in one end cap to
allow the unobstructed passage of the electron beam. The
sample and mounting disc are insulated from the other end cap
although the iris and all probe motion mechanisms are elec-
trically connected to the enclosure. The current in the lead
connecting this enclosure (total charge collector) to ground

measures the current of emitted particles. In this configuration, the retarding potential analyzers cannot be used because the sample is mounted perpendicular to the incident electron beam.

In an attempt to locate the site of particle emission during a discharge event, the surface voltage probe was replaced by a two-sided charge collector. The collector facing the sample is isolated from the remainder of the system permitting a measure of the particles emitted by the sample area directly below the collector. The outer side is connected with the total charge collector to measure the charge emitted by the unobstructed surface (Fig. 4).
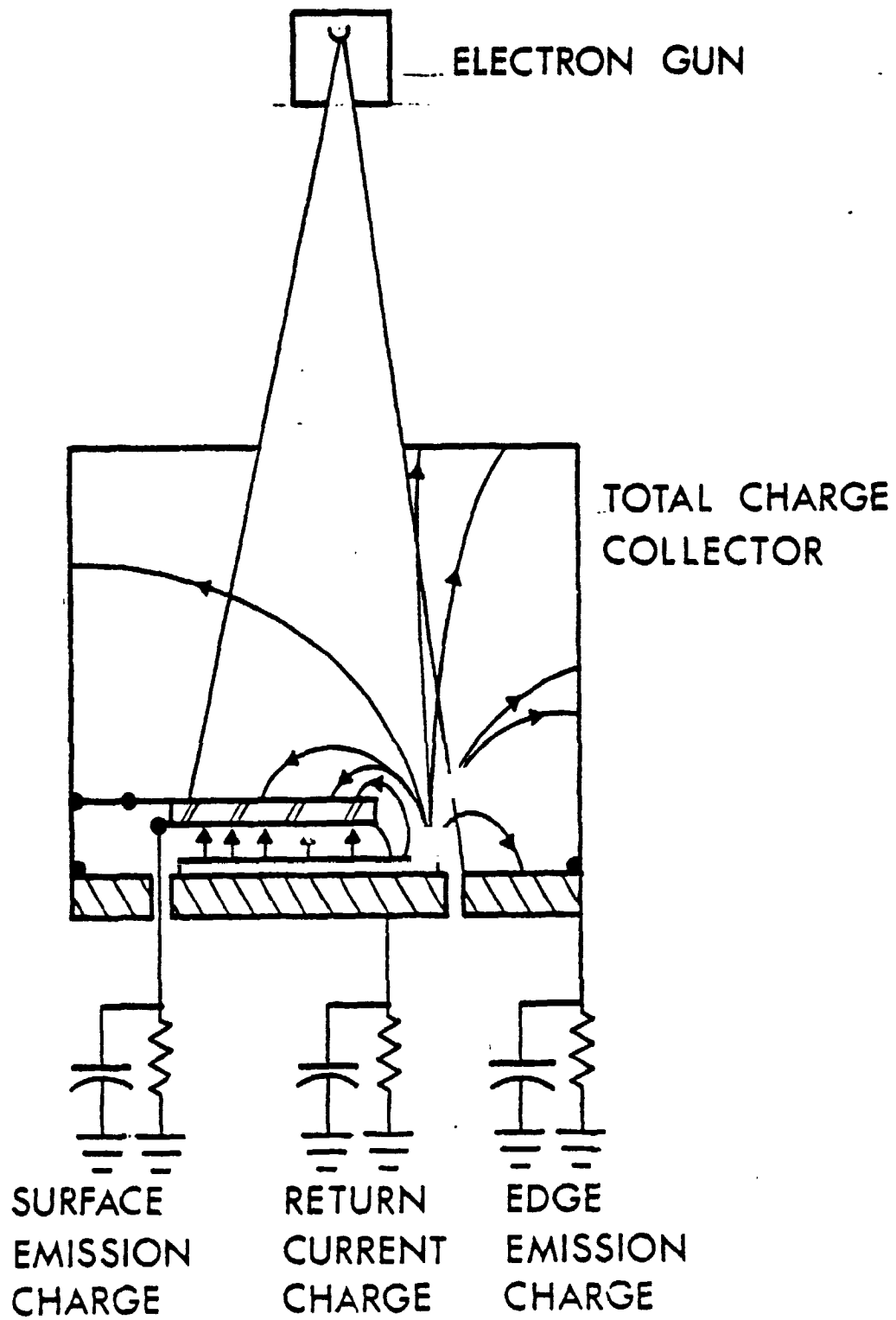
ELECTRON GUN

TOTAL CHARGE
COLLECTOR

SURFACE
EMISSION
CHARGE

RETURN
CURRENT
CHARGE

EDGE
EMISSION
CHARGE

Figure 4. System for measurement of charge balance
and emission site location.

MEASUREMENT TECHNIQUES AND RESULTS

The measurements conducted during the course of this
project can be placed in three main categories: 1) Breakdown
voltage measurements, 2) Discharge path measurements, and
3) Particle emission measurements. In this section all data
pertaining to these measurements are presented.

Measurements of the breakdown voltage were first made for
previously unirradiated samples with the edges shielded. Surface
potentials were inferred from the measured electron beam voltage.
To ascertain the potentials required to reach the breakdown
threshold, the sample was irradiated first at a beam voltage
substantially below the anticipated threshold. The beam voltage
was then increased in 2 kV increments allowing time for equili-
brium to be attained at each voltage. The thresholds are plotted
against sample thickness in Figure 5 and demonstrate a reason-
ably linear correlation between thickness and breakdown voltage.[11]
In addition, the history of the breakdown voltage occurring on
a single 75μ sample (Fig. 6) demonstrates a wide variation.
For the particular example shown, the initial breakdown voltage
is 26 kV decreasing to 14 kV after twenty breakdowns. It is
noteworthy that the breakdown voltage does not stabilize at
any particular value.

Early measurements of breakdown voltages with exposed
edges indicated that the threshold is substantially reduced;
e.g., 14 kV threshold for a 125μ sample as opposed to 34 kV
for a 125μ sample with edges shielded. Subsequent measurements
indicate that the threshold depends upon which edge is exposed.
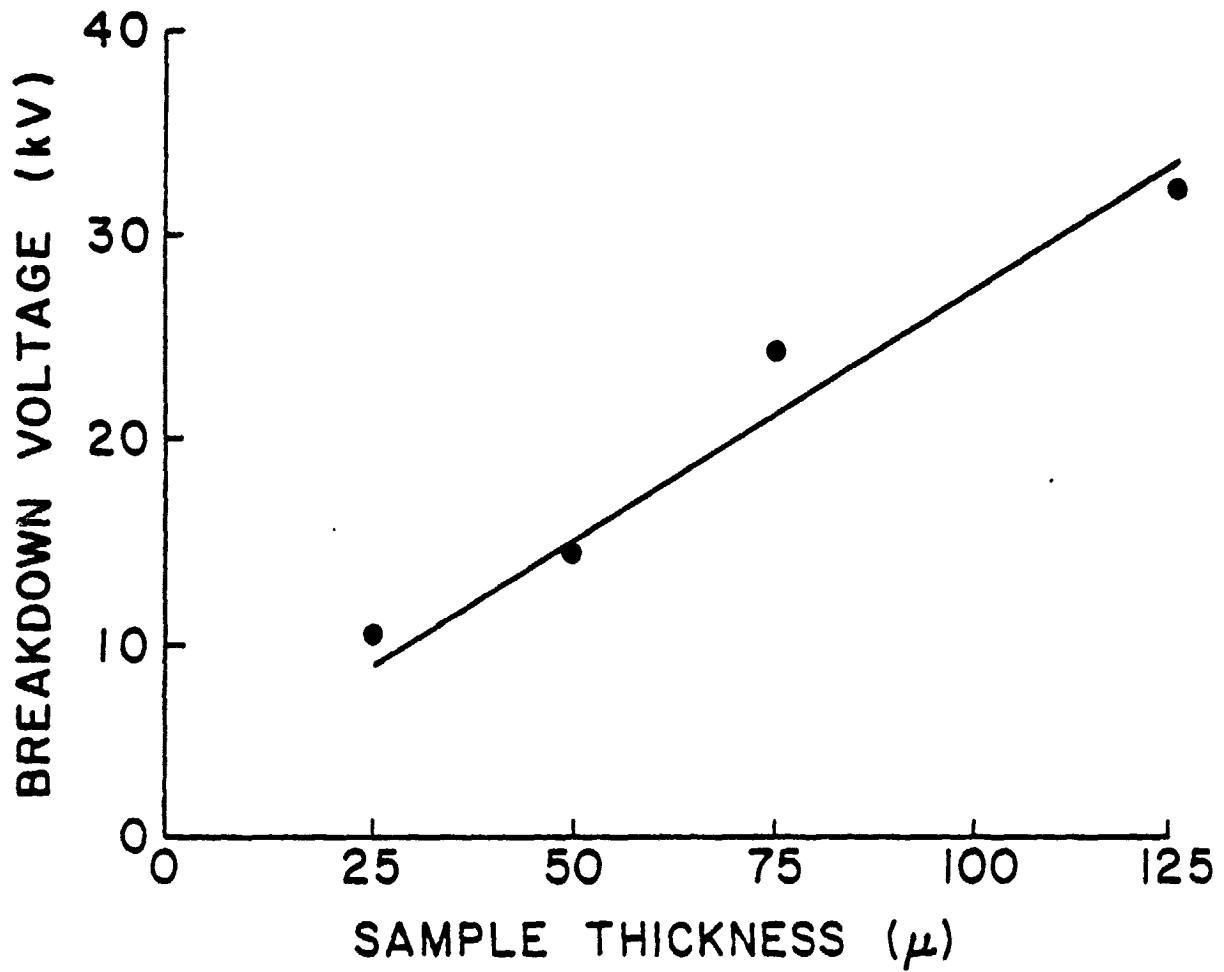This was first noted in a 125μm sample with a pre-applied

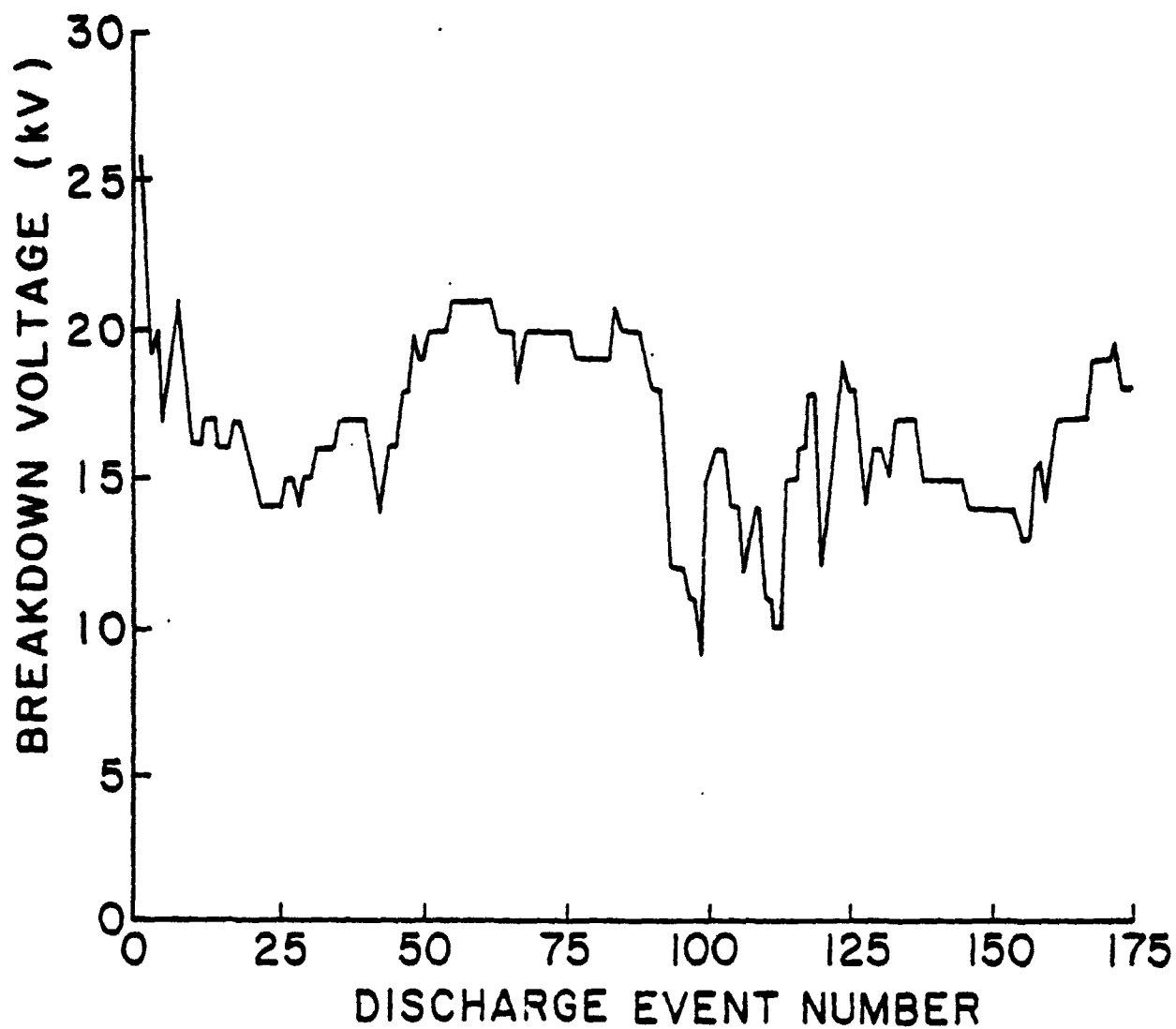Figure 5. Electrical breakdown of silver-backed Teflon samples.

Figure 6.   History of breakdown voltage for 75μ
           silver-backed Teflon sample.

conductive adhesive (NASA roll #2696). A sample was installed with an exposed edge along the length of roll. The breakdown threshold was consistently measured to be 30-34 kV. A new edge was then exposed perpendicular to the previously exposed edge. The threshold dropped to the range of 16-24 kV, indicating an anisotropy in breakdown threshold dependent upon some aniso-tropy in the material itself.

Similar measurements with a 75μm sample (NASA #C-65425-C) demonstrated a threshold of 20-24 kV for one edge and a threshold of 8-14 kV for the perpendicular edge.

The paths followed during discharge events have been inferred by observing the luminescent traces occurring during a discharge, the material damage resulting from these discharges, and the residual charge on a sample after the occurrence of a discharge.

The observed luminescence for puncture discharges generally exhibited a classical Lichtenberg pattern across the sample surface terminating in bright spots on the sample. The observed luminescence for edge breakdowns generally consisted of a series of linear and parallel streamers. If the exposed edge is para-llel to the length of the roll (high threshold voltage values), the luminous paths are parallel to the exposed edge. On the other hand, if the exposed edge is nearly perpendicular to the length of the roll (low threshold voltage values), the parallel luminous paths all terminate at the edge at some fixed angle. In all cases, the luminous paths were found to be parallel to the length of the roll. This linearity is in sharp contrast to

the Lichtenberg patterns of the puncture breakdowns.

Material damage on the samples with shielded edges following an electrical discharge has been studied using an optical microscope and a scanning electron microscope (SEM). The optical microscope reveals information about sub-surface damage as well as surface damage, whereas the SEM is used for high resolution surface studies. The photographs in Figure 7 reveal a hole through the dielectric material to the grounded silver-backing resulting from the discharge current flow. In addition, this microscopic investigation reveals the existence of filamentary surface tracks which terminate at the holes as in Figures 7a and 7b. These material damage tracks are similar in form and appearance to luminous Lichtenberg streamers observed on the surface during the discharge, although no direct comparison has been made. The tracks in the Teflon appear to be the results of currents which flow through the Teflon parallel to the surface during the discharge of the sample. The process of discharging the sample by currents flowing underneath the sample surface is consistent with puncture sites where filamentary material damage has occurred as in Figures 7a and 7b. In Figure 7c, a current filament is seen to surface a number of times before reaching the main discharge channel.

Using the optical microscope, the depth of these channels was found to be 8-12μm. The microphotographs of the discharge sites dramatically demonstrate the material damage resulting from the discharges on the sample. It is evident that the
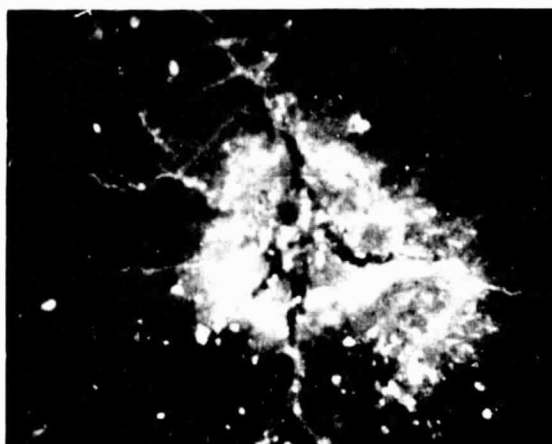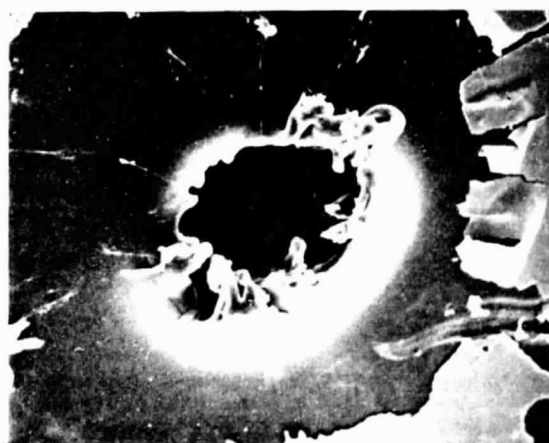
a. Optical micrograph showing subsurface filamentary structure. (75 X)

b. Scanning electron micrograph of breakdown site shown in 4a. (190 X)
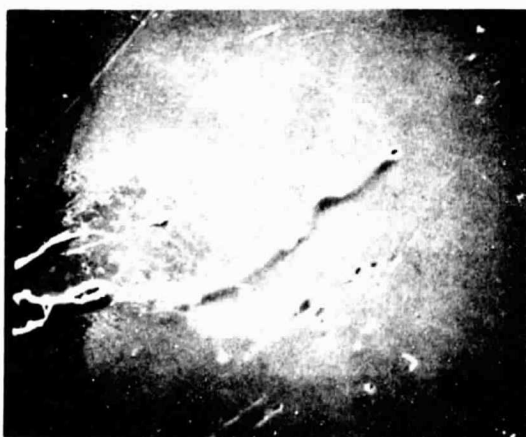
c. Scanning electron micrograph of filamentary structure near breakdown site shown in 4a. (225 X)

d. Scanning electron micrograph of damage to silver side. (225 X)

Figure 7. 75μ silver-backed Teflon sample irradiated at 26 kV with a beam current density of $\sim$ 1 nA/cm^2.

energy in the current channel is sufficient to rupture the
channel as in Figure 7 and to eject molten Teflon from the
puncture site. In addition, there is appreciable silver loss
from the grounded silver-backing as seen in Figure 7 as well
as extensive melting and ejection of material from the dis-
charge sites.[12]

The Lichtenberg damage patterns occur infrequently in
Teflon with the more common damage being only the puncture
itself.

The material damage in exposed edge breakdowns differs
significantly from the punctures seen previously in shielded
edge experiments. In these cases, linear damage tracks are
seen on or below the surface which are colinear with the
luminous tracks. Again, less material damage is seen than
would be expected if every luminous track was accompanied
by a damage track.

An additional diagnostic technique used in studying edge
breakdowns is the surface potential probe. The surface potential
profile before the breakdown occurs is shown in Figure 8,
and after the breakdown event in Figure 9, from which the
residual charge and discharge areas can be inferred. Here
the discharged regions, shown stippled in Figure 9, are roughly
linear in nature corresponding to the linear luminescence and
damage tracks.

The characteristics of the particles emitted during puncture
discharges through the dielectric surface were measured using
the three particle collectors (Faraday cup, RPA and HERPA)
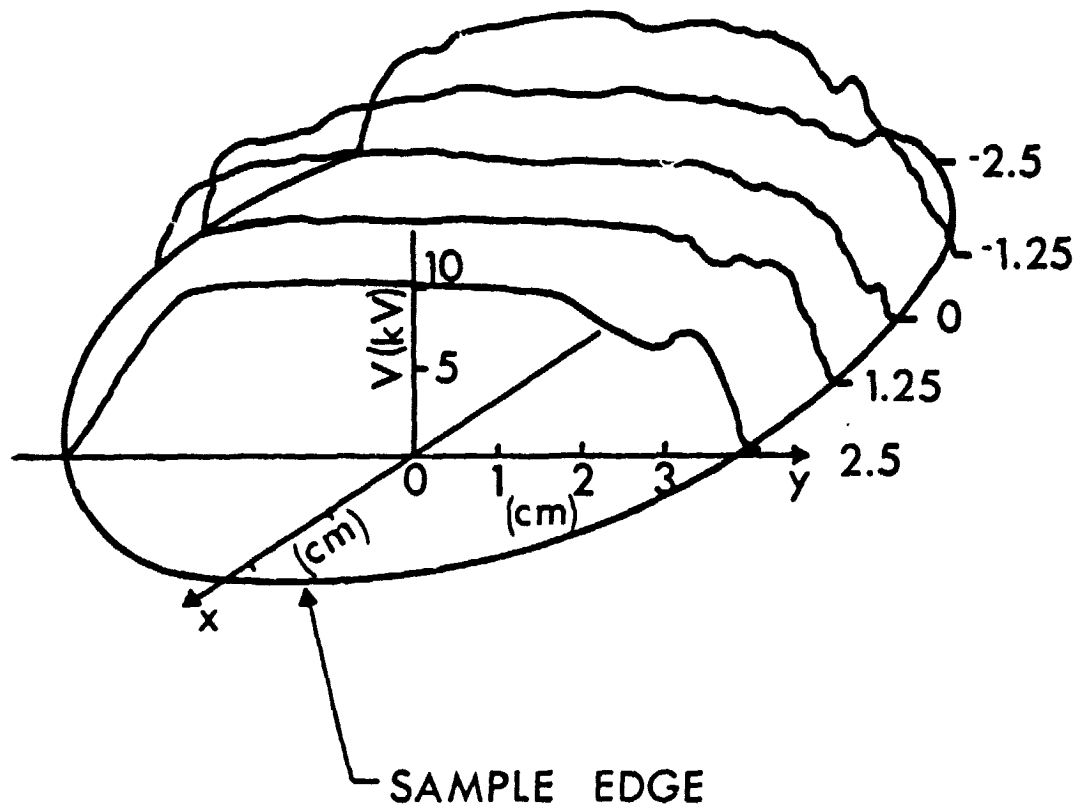described in the previous section.

Figure 8. Surface potential profile (kV) prior to discharge. The 'length of roll' direction is along the X axis.
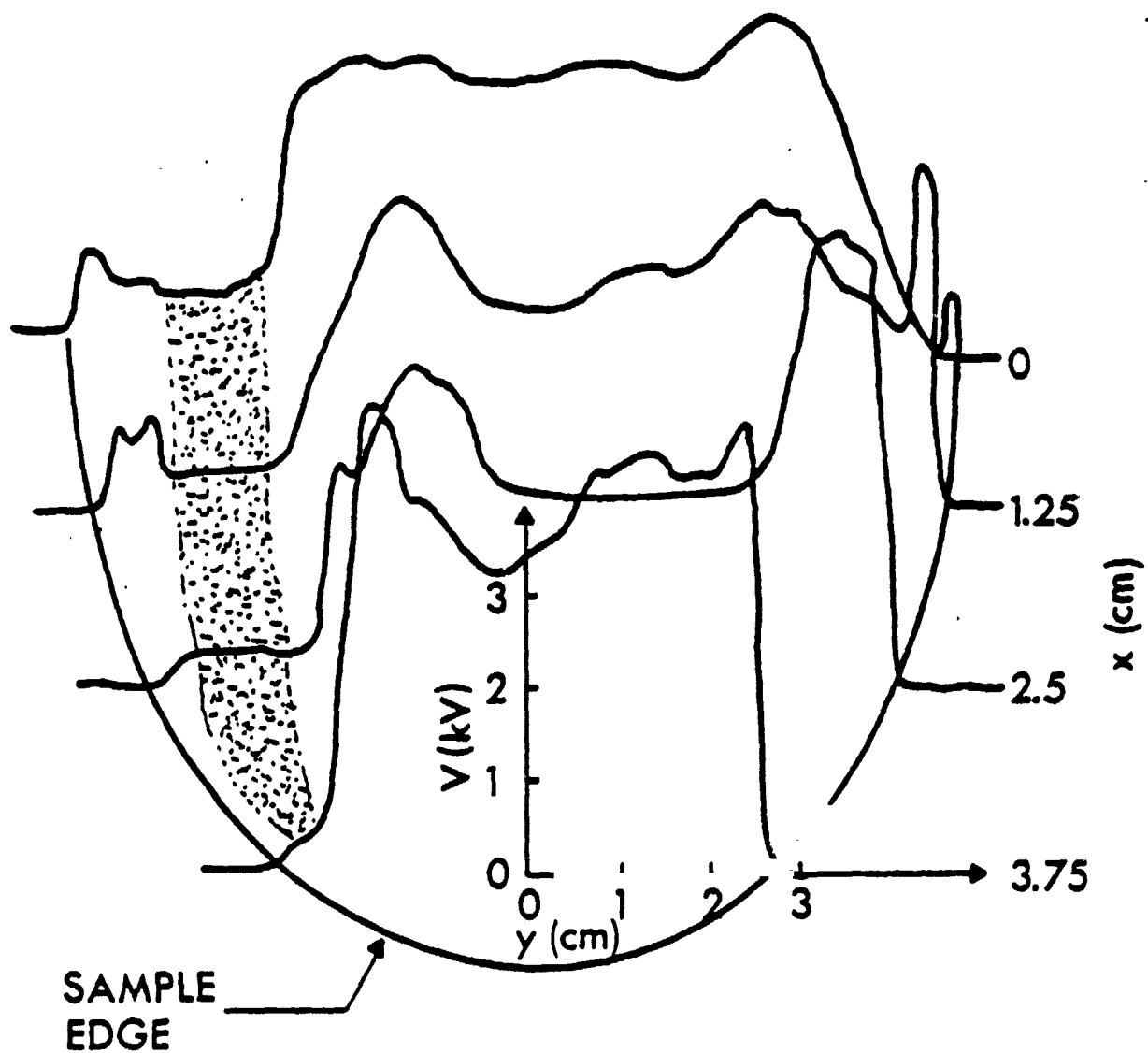
Figure 9. Surface potential (kV) profile after discharge for half the sample surface showing a linear charge depleted region (stippled) along the 'length of roll' direction (X axis).

The emission is made up of two distinct bursts of particles: an early electron pulse and a later plasma pulse[12] (Fig. 10). For all discharges an early electron pulse is observed having a duration of up to 600ns. On the other hand, the plasma pulse occurs infrequently and such occurrences appear to be related to the establishment of new puncture discharge sites in the dielectric.[11] The plasma pulse persists for 1-5μsec. To measure the angular distribution of emitted particles, the RPA was appropriately biased and a number of discharges recorded at each angle. Because of the variation of total emitted flux observed from one discharge event to another, the Faraday cup was maintained in one position and the observed particle fluxes were used to normalize the RPA measurements. Figure 11 shows the angular distribution of the positive ion component of the plasma pulse. It can be seen that the emission is strongly directed normal to the sample surface. Figure 12 shows the angular distribution of the early electron pulse. Again, the electrons are emitted nearly normal to the dielectric surface.

To measure the energy of the particles constituting the early electron and plasma pulses the HERPA and RPA, respectively, were used. In both cases the detectors were positioned with the axes normal to the dielectric surface to achieve maximum signal strengths. The collectors were biased appropriately to collect either positive or negative particles and the retarding grid incremented to sweep the energy range of the particles. As before the data represent a composite of data collected over a number of discharge events normalized to the Faraday cup
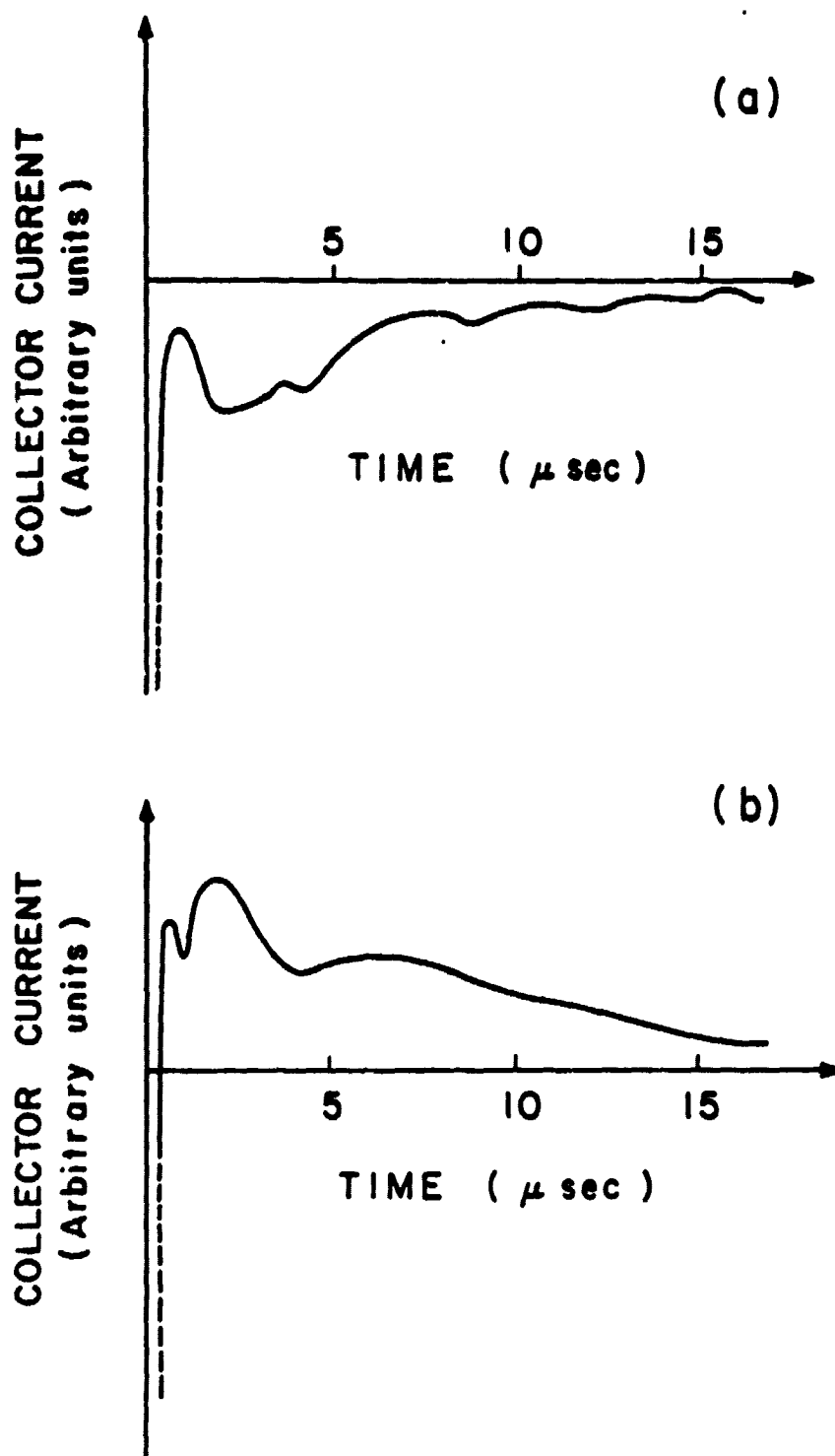
Figure 10. Oscilloscope traces of Faraday cup current:
(a) Faraday cup biased to collect negative
particles.

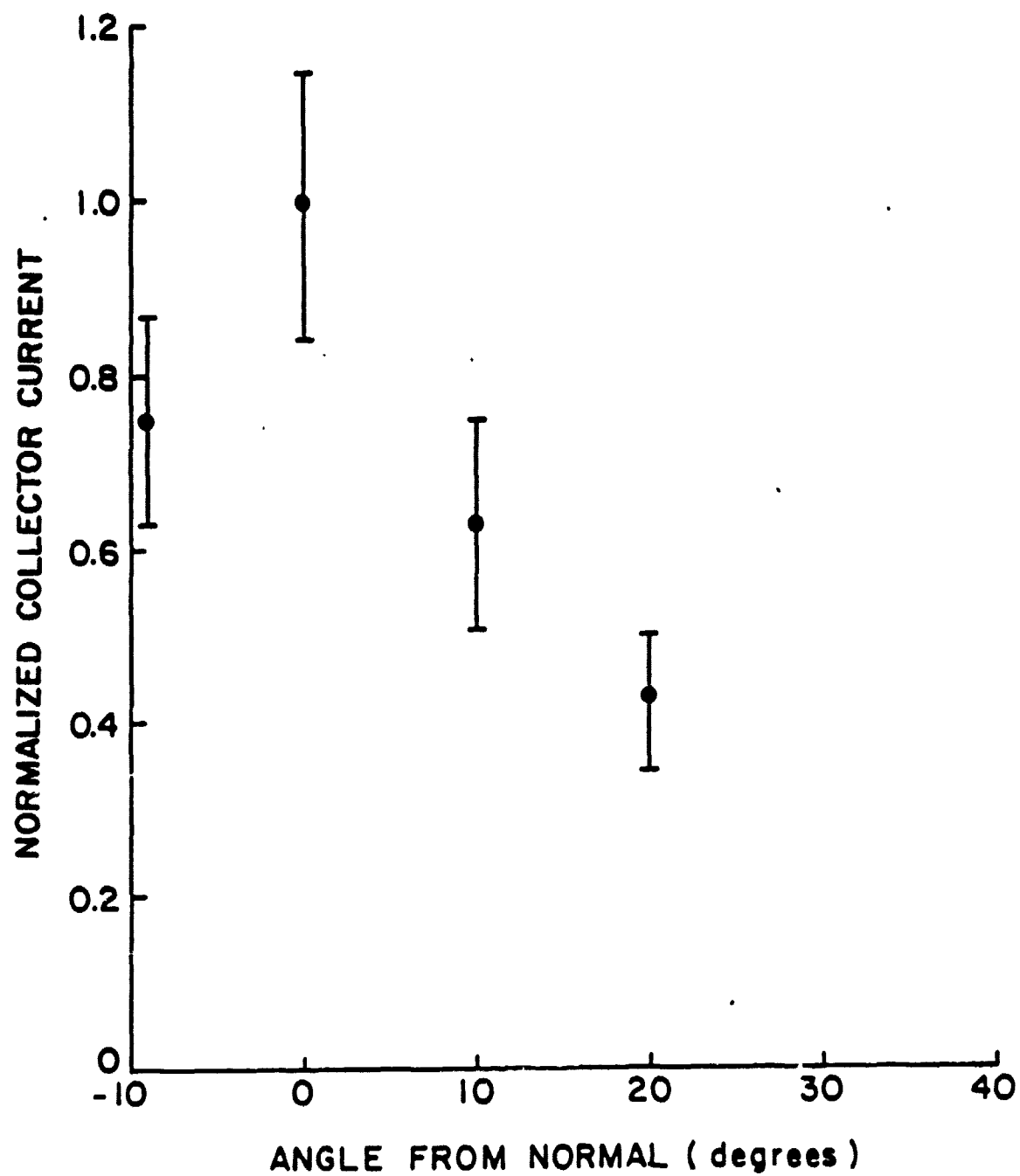(b) Faraday cup biased to collect positive
particles.

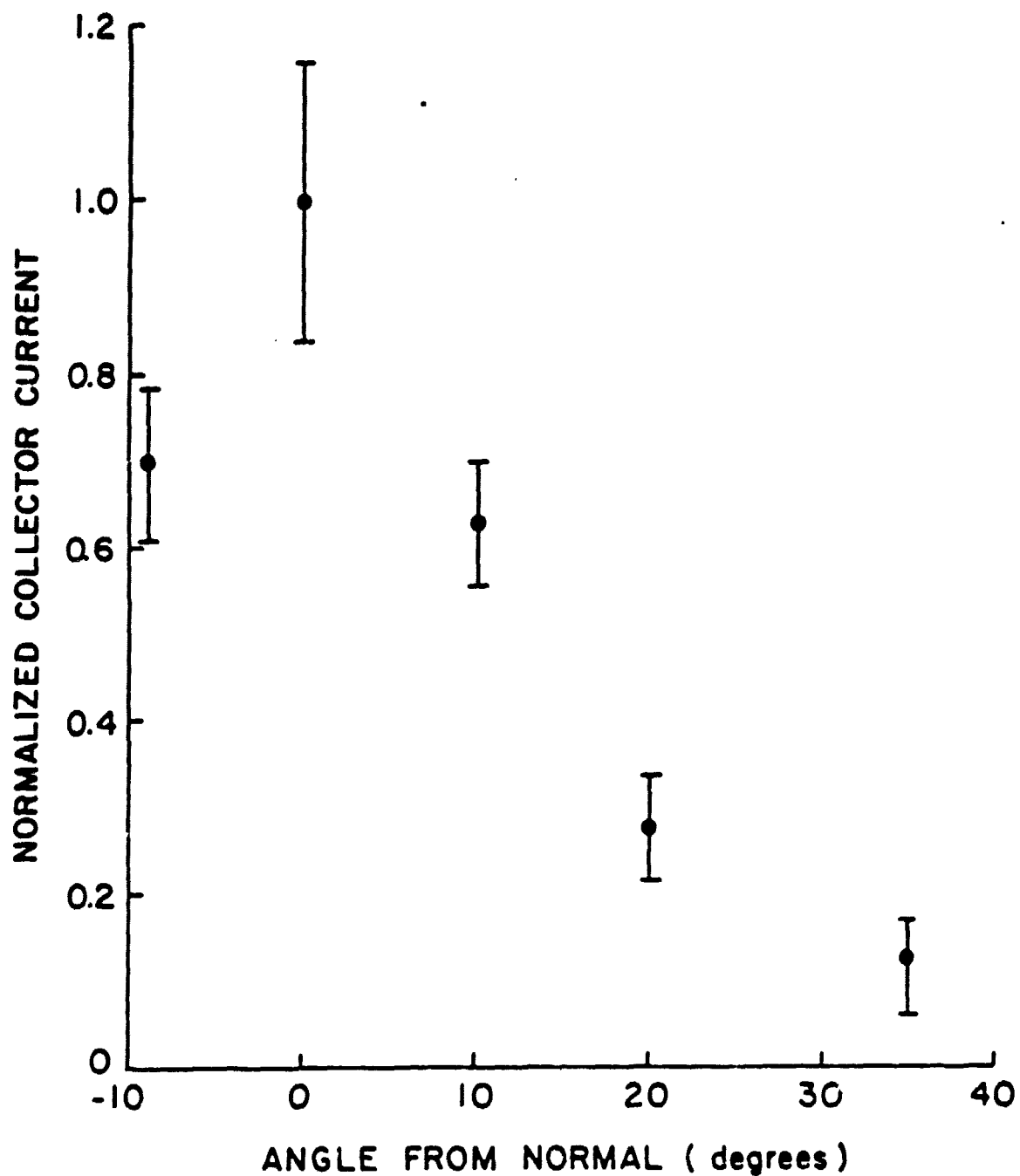Figure 11. Angular distribution of positive ions in the plasma pulse emitted during a discharge.

Figure 12. Angular distribution of electrons in the early burst of electrons emitted during a discharge.

current. In Figure 13 RPA collector current at various

retarding potentials is shown for the ion component of the

plasma pulse. The positive particles have a minimum energy

of 30eV and an average energy of $\sim$70eV. A similar profile

for the negative component was not obtained because of the

limited resolution ($\sim$1V) of the retarding potential analyzer.

Nevertheless, the measurements do indicate electron energies

much less than 1eV. These observed electron and ion energies

are consistent with the fact that particles with the same

velocity have an energy ratio equal to their mass ratio.

Collector current profiles for the early electron pulse

were obtained using the high energy retarding potential analyzer.

Due to large variations in the breakdown voltages for a given

sample, these profiles were constructed by noting the breakdown

voltage for each discharge and then grouping the data with the

breakdown voltage as a parameter. The variation in collector

current with retarding grid voltage was determined at various

times during the discharge. Figure 14 shows the current

profiles at the peak of the emission pulse for various break-

down voltages. Figures 15 and 16 show time resolved collector

current profiles for 16kV and 20kV discharge events, respectively.

Differentiation of the curves in Figures 14, 15, and 16 with

respect to grid voltage to obtain the energy distribution of the

emitted particles has not been done because of the limited

number of points and scatter in the data. The curves themselves

provide information about the maximum energy and energy spread

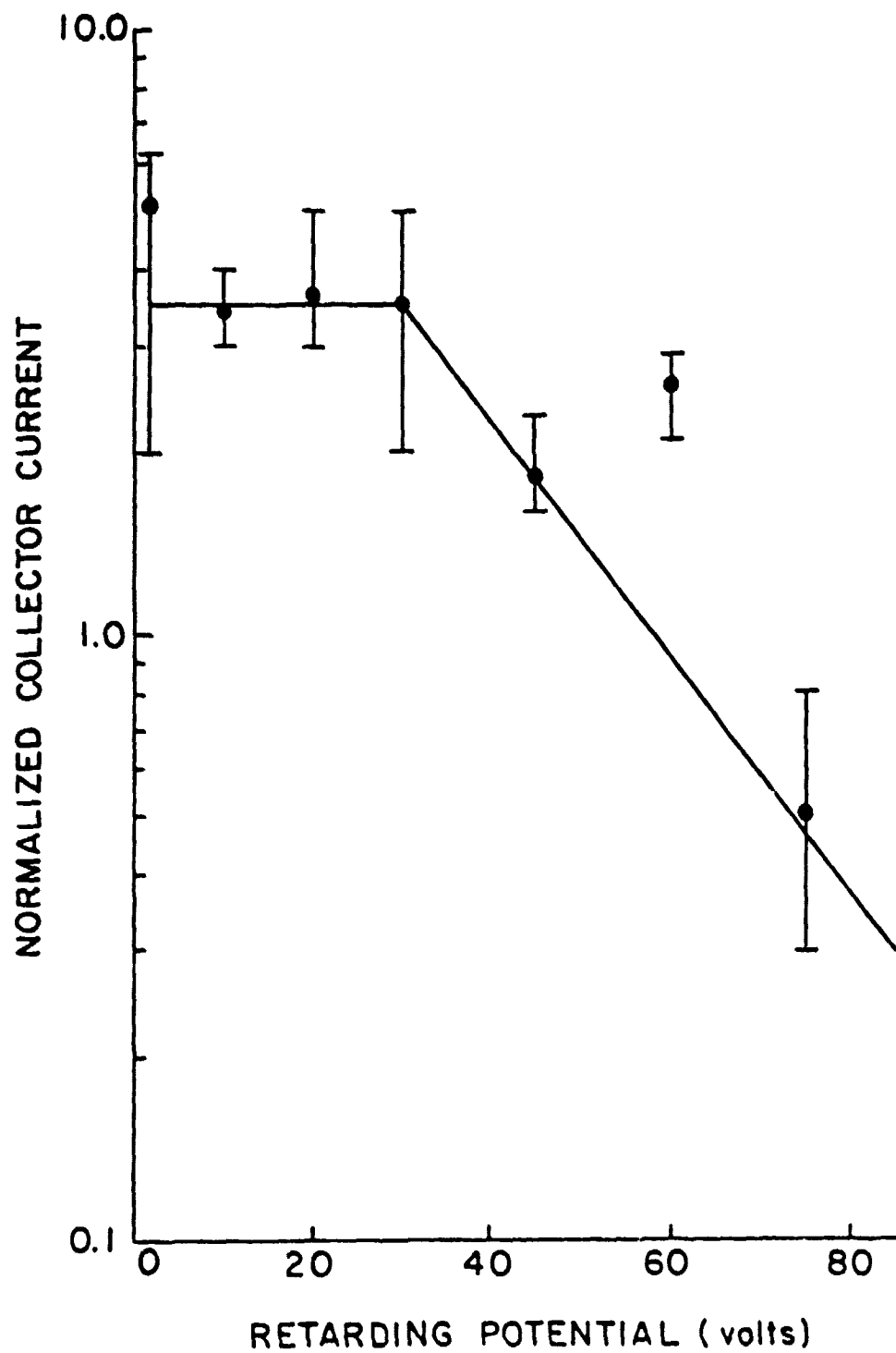in the emitted particles at various times during the discharge

Figure 13. Collector current for positive ions measured with retarding potential analyzer.
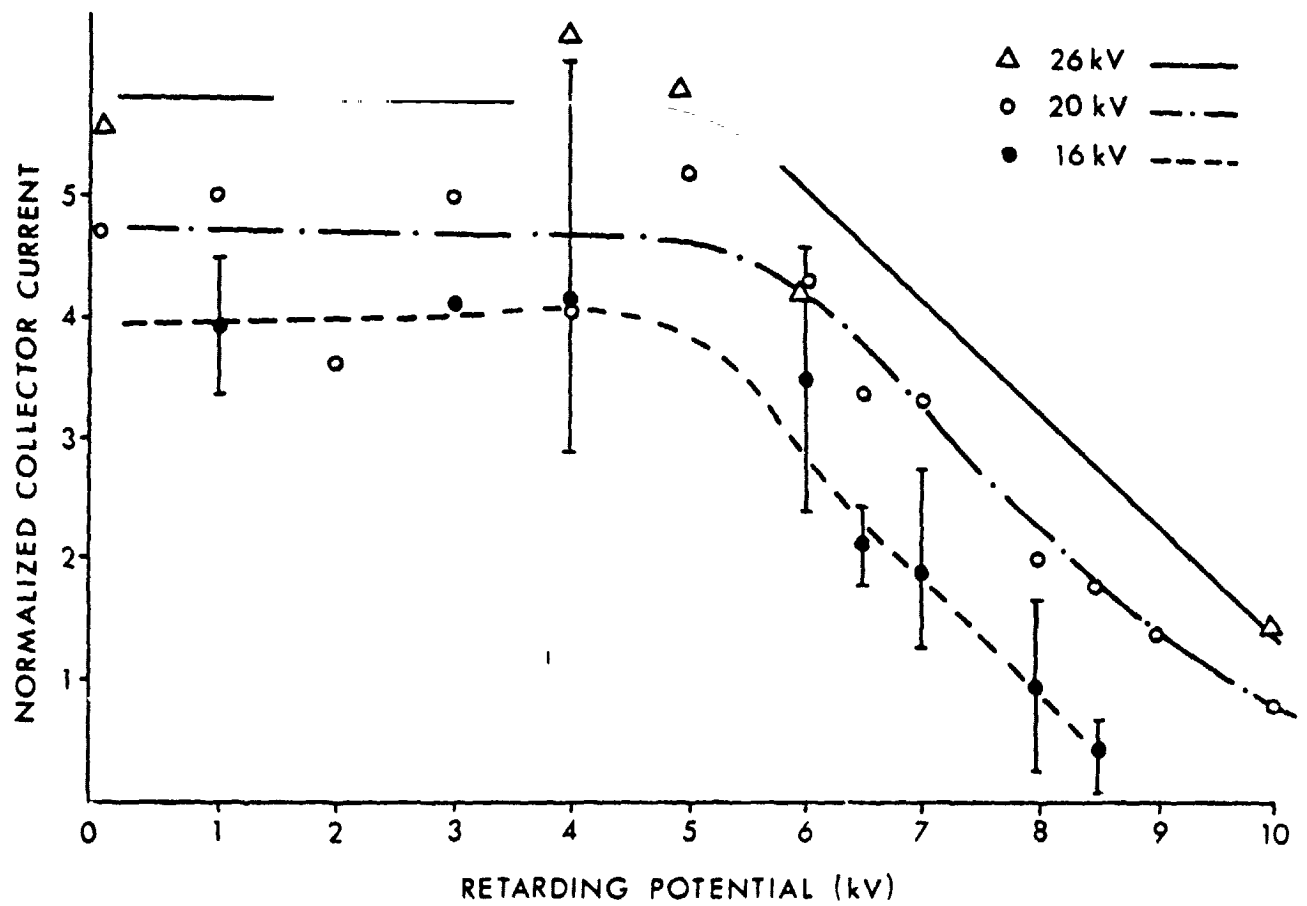
Figure 14. Variation in electron energy with breakdown voltage at peak particle emission.
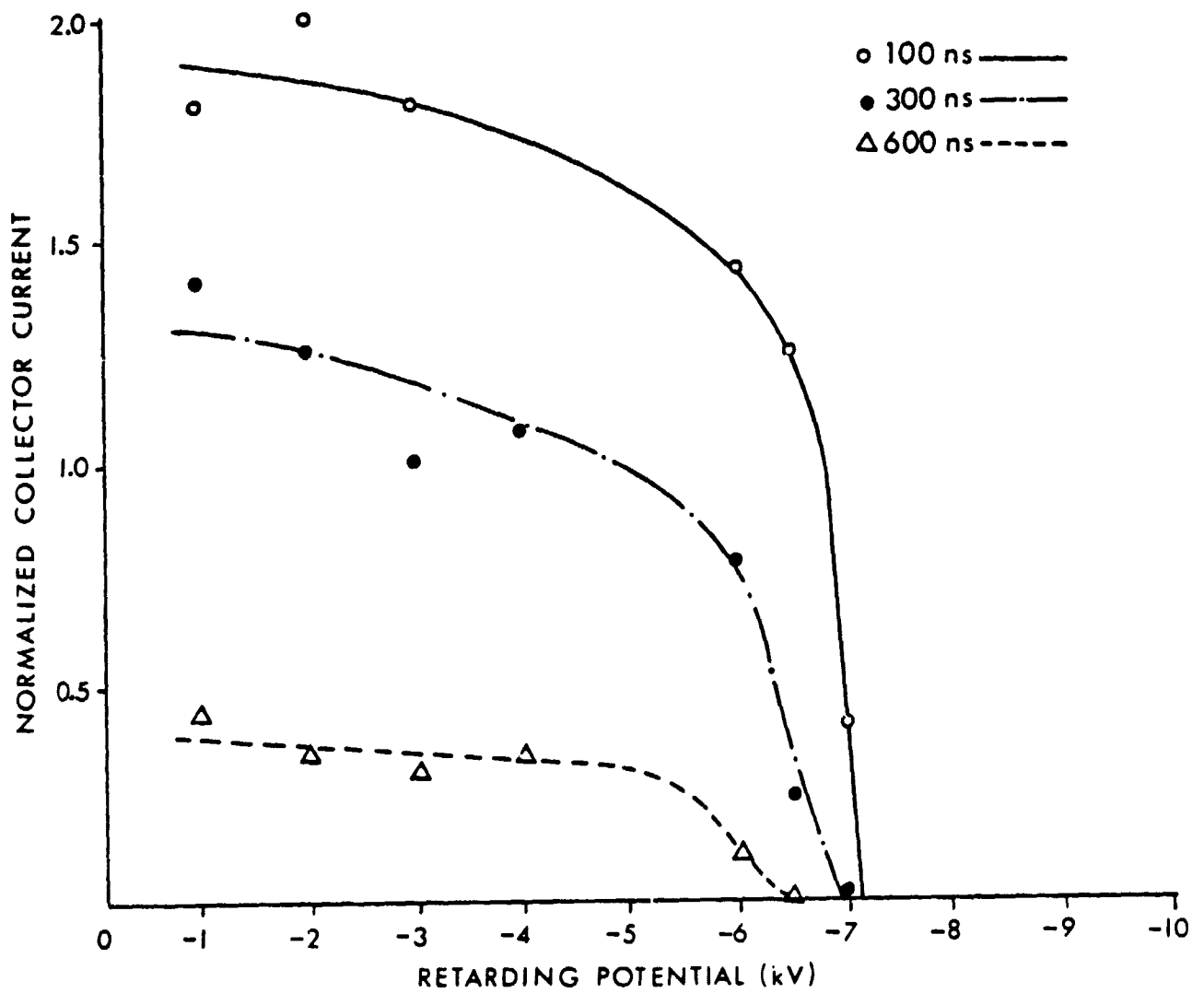
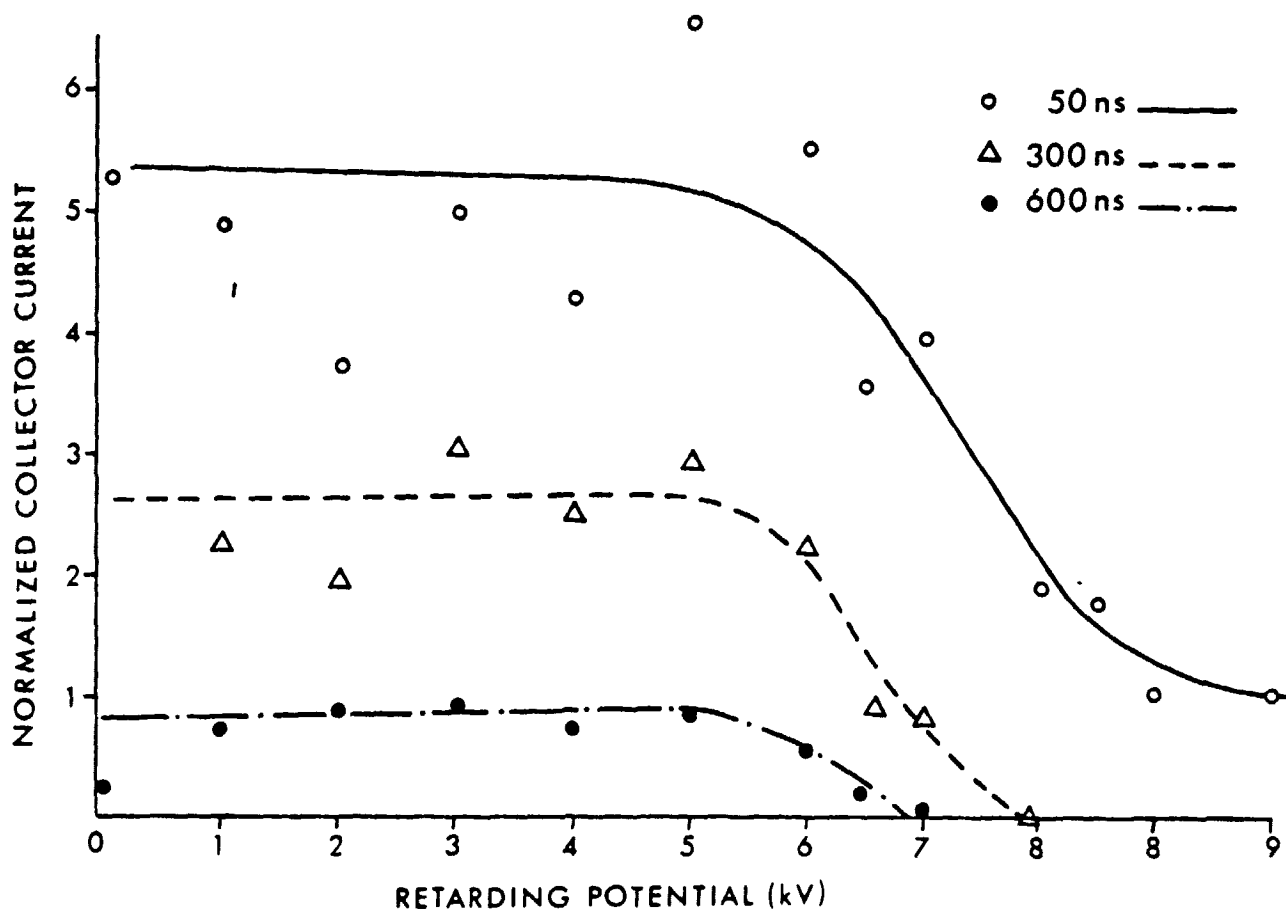Figure 15. Variation in electron energy with time for 16kV breakdown.

Figure 16. Variation in electron energy with time
fcr 20 kV breakdowns.

process. In all the distributions, the minimum electron energy is ~5keV with the maximum extending to ~10keV.

In Figure 17 the maximum observed electron energy is plotted versus the breakdown voltage and a linear relationship is seen to exist. It should be noted, however, that the maximum electron energies are considerably less than those that would be derived from the electron beam voltage at breakdown indicated on the abscissa.

For edge breakdowns the plasma pulse was not observed. However, again the early high energy electron pulse was observed and the energy content measured. Figure 18 shows the collected particle current as a function of the retarding potential for a breakdown voltage of -8kV. An extrapolated maximum energy of 5 keV is obtained from this graph. Adding this point to the graph of maximum energy vs. surface potential (Fig. 17) shows that the relationship observed in shielded edge breakdowns is maintained for the edge breakdown process.

Another aspect of particle emission measurements is the determination of the scaling of emitted charge and return current with area. Using the HERPA biased to collect all electrons, the emitted charge was measured as a function of exposed sample area. As can be seen in Figure 19, the charge scales with the exposed area. Similarly (Fig. 20), the return current also scales with the area for peak return current spikes.

Charge balance during a discharge event was studied to determine if the emitted particles could account for the return current pulse. The emitted charge was determined by integrating the current pulse of the two emitted charge detectors (surface
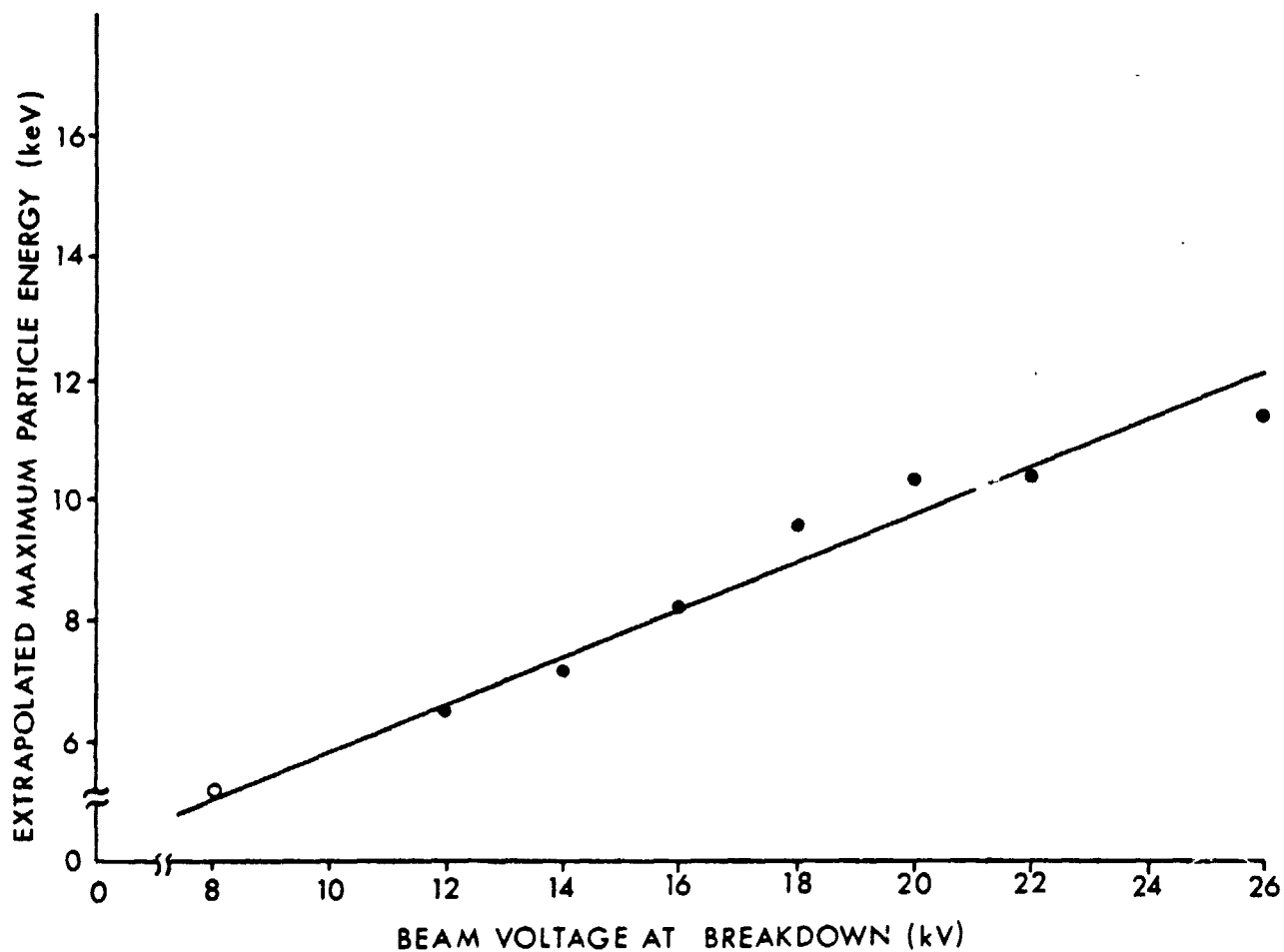
Figure 17. Maximum electron energies inferred by
extrapolation from curves in Figure 14
for shielded edge breakdowns (solid dots)
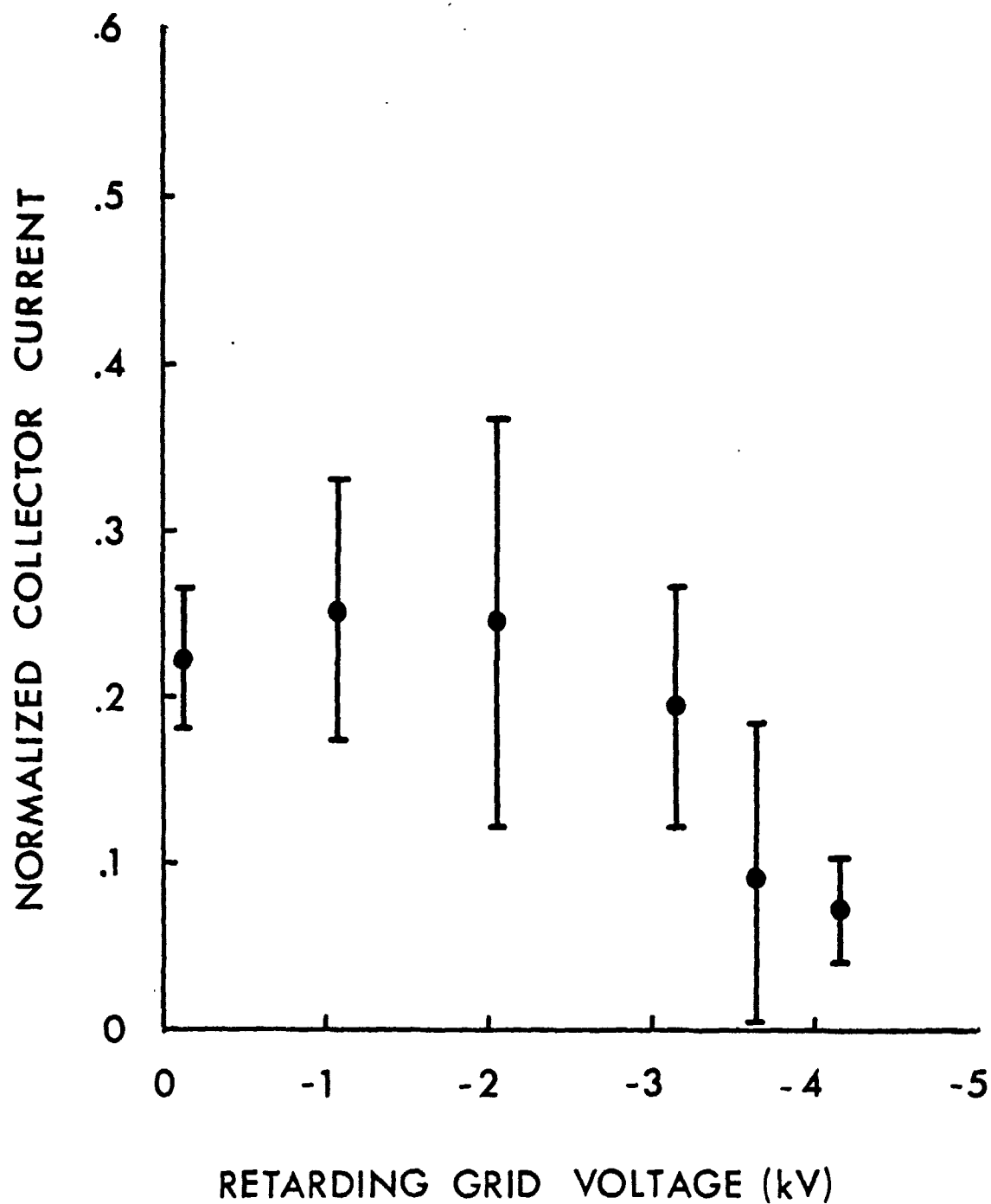and from curves in Figure 18 for edge
breakdowns (open circle).

Figure 18. Collector current for electrons emitted during edge breakdowns.
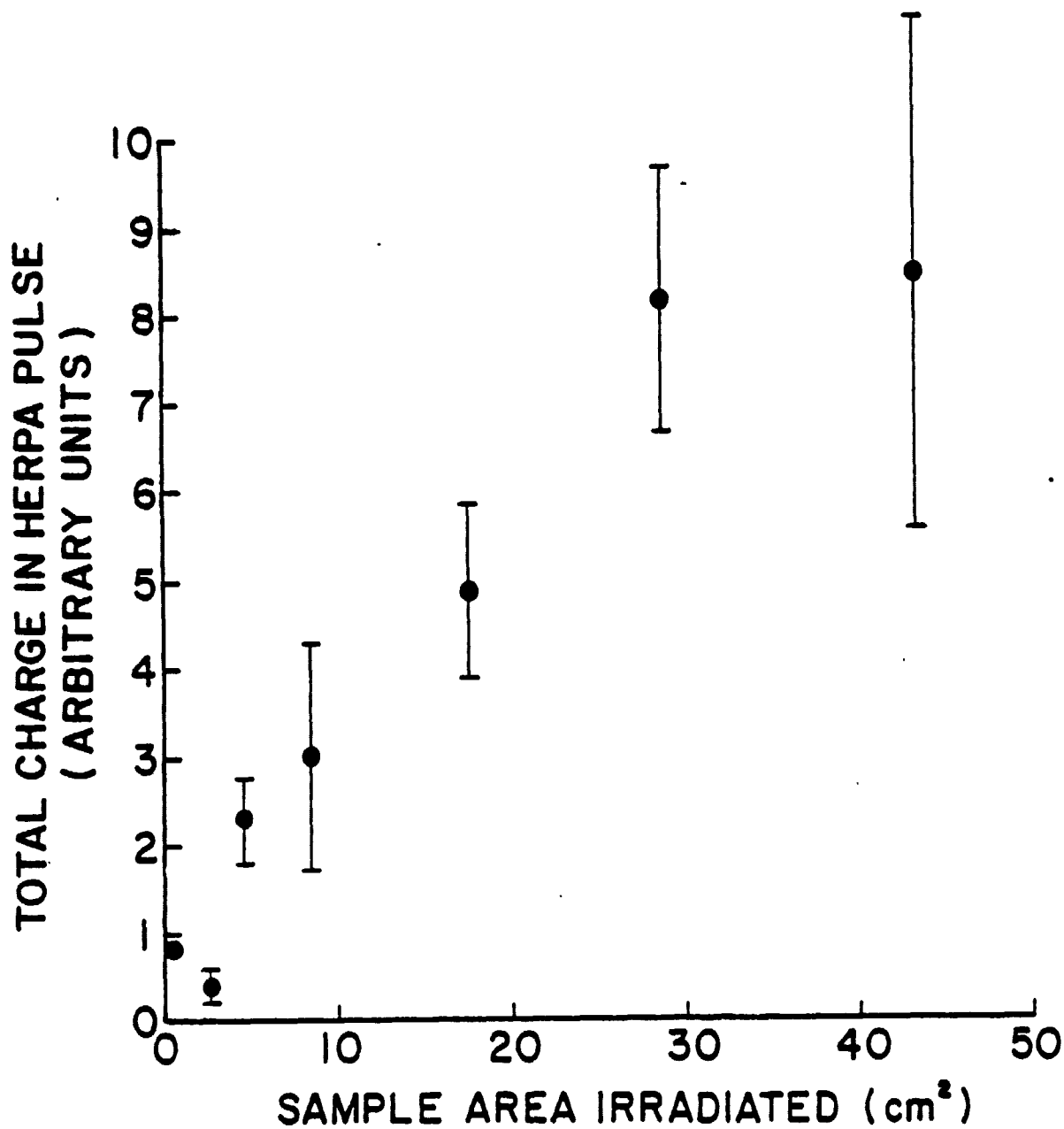
Figure 19.   Charge contained in early electron pulse for various sample areas irradiated.
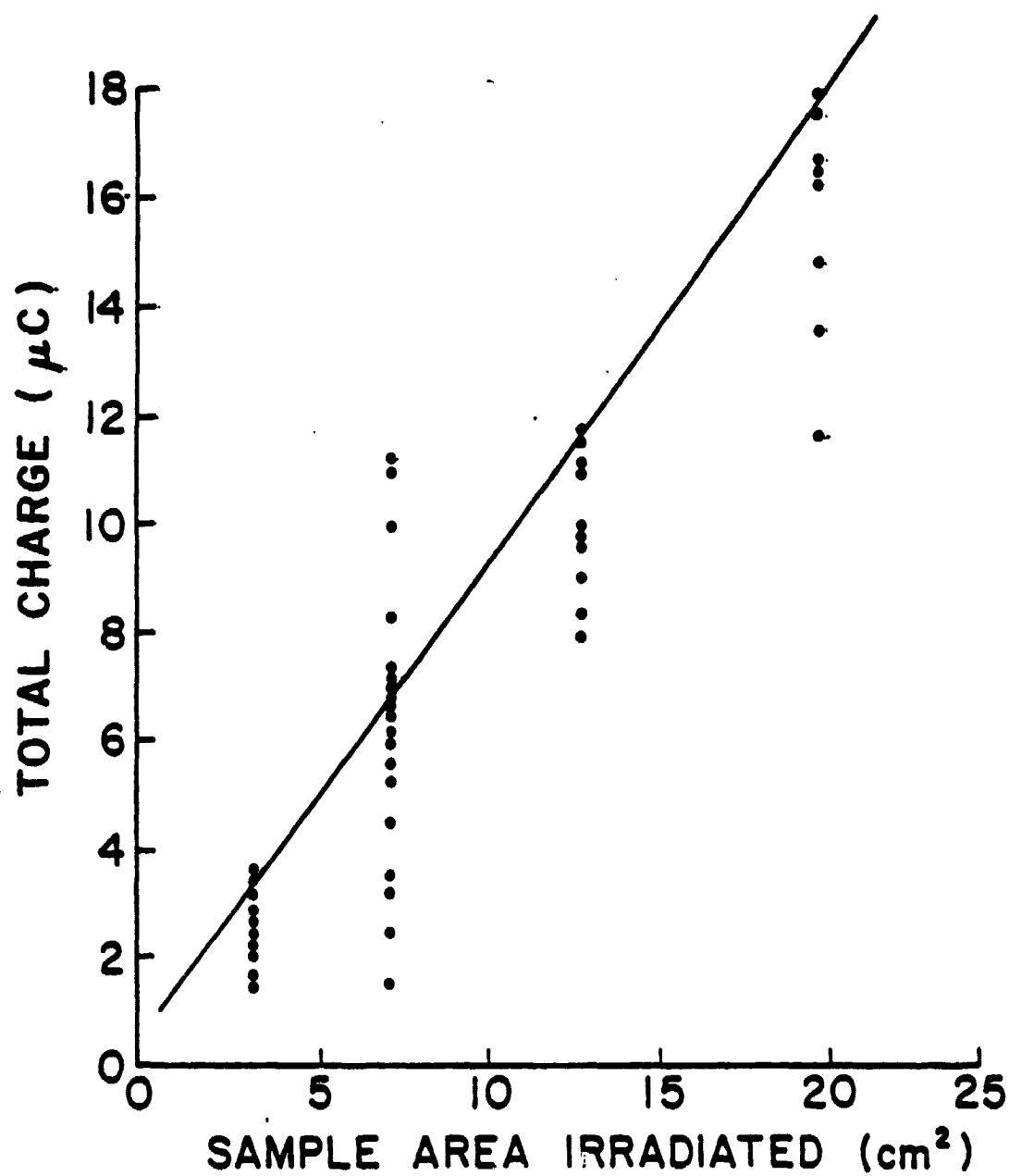
Figure 20. Charge contained in return current pulse
for various sample areas irradiated.

and edge) in Figure 4. The accumulated charge of·these two
detectors is found to be 90 ± 2% of the total charge in the
return current pulse. These measurements indicate that the
return current is a result of the emitted electrons, since
the aperture in the total charge collector required to emit
the irradiating beam will allow some particles to escape
undetected. The aperture area is about 10% of the cross-
sectional area of the charge collector.

The total charge detector shown in Figure 4 was designed
to distinguish between particles emitted from the breakdown
site (sample edge in this case) and particles that might be
emitted from the overall sample area in an attempt to locate
the site of particle emission. The procedure is to first
charge up the sample. For this phase of the experiment, the
two-sided surface emission detector in Figure 4 was moved to
the right so that a strip 1.2cm wide along the edge was shielded
to reduce the possibility of breakdown. The detector was then
moved to the left in Figure 4 to cover the area previously
charged and expose a strip 1.4cm wide along the edge. This
newly exposed surface was irradiated until an edge breakdown
discharged the sample. Since the distance between surface
emission probe and sample surface is small compared to the
dimensions of the shielded area, particles emitted by sites on
the shielded surface would be collected by this probe; the
particles emitted by the exposed edge area would be predomi-
nantly collected by the total charge collector. Measurements
indicate that the surface emission probe collects 30% of the
emitted charge while covering 80% of the sample surface. No

measurements were made to date to indicate what fraction of
the shielded surface was discharged.

DISCUSSION OF RESULTS

The measurements of the beam voltage required to initiate a breakdown in a previously unirradiated sample together with the observations of the luminous discharge pattern and material damage characteristics provide information about the physical breakdown process and subsequent discharge of the sample surface. At least two distinct discharge processes are indicated by the results.

The observations of a threshold breakdown voltage linearly proportional to sample thickness as shown in Figure 5 indicate that bulk properties of the dielectric determine the initial breakdown of a dielectric sample with edges shielded from the electron beam. The value of the dielectric breakdown strength (8×10^7 V/m) predicted by the slope of the straight line in Figure 5 is within the range of values 28×10^7 V/m to 2.8×10^7 V/m for Teflon thickness in the range of 25 to 125μm specified by the manufacturer.[13] The beam voltage measurements are a meaningful measure of the breakdown characteristics even though the equilibrium surface voltage was not measured. Stevens et al[14] have shown that the difference between these two quantities is a fixed value of 1.8kV that is associated with the net accelerating voltage required to establish a secondary emission coefficient of unity. The straight line in Figure 5 intercepts the voltage axis at a value of 2.5kV, which is in reasonable agreement with the reported value of 1.8kV for the measured offset. Different initiation and discharge processes are implied by the observed variation in threshold voltage shown in Figure 6.

In the case of shielded edge breakdowns, the similarity observed between the luminous patterns and the material damage gives a physical picture of the breakdown processes. It is reasonable to assume that the punctures observed in the sample and the bright spots in the Lichtenberg patterns are the initiation points of the breakdown where the electric field in the material exceeded the local dielectric strength associated with a material defect. The presence of material damage tracks at a distance below the sample surface corresponding to the range of the incident electrons indicates that the dielectric is discharged by currents flowing beneath the surface in channels formed by vaporization and ionization in certain cases. Since many discharges occur without the Lichtenberg pattern of material damage, the electrical paths may be established by other processes such as electron-hole pair formation. These observations are consistent with those reported in the literature (Fogdall et al[15] and Balmain and Dubois[16]).

The microphotographs of the discharge sites dramatically demonstrate the material damage resulting from the discharges on the sample. It is evident that the energy in the current channel is sufficient to rupture the channel as in Figure 7b and to eject molten Teflon from the puncture site. In addition, there is appreciable silver loss from the grounded silver-backing as seen in Figure 7d. Two consequences of importance to spacecraft performance are immediately evident. First, the repeated discharges observed at individual sites can lead to deterioriation of thermal control surface efficiency because of silver losses. Secondly, the material ejected from the

discharge sites is a source of contamination of the spacecraft and its environment.

The luminous discharge paths and threshold voltage measurements on samples with edges exposed to the irradiating beam indicate the presence of material anisotropy in Teflon.

The straight parallel lines characteristic of the luminous discharge patterns and the material damage in these edge breakdowns contrast sharply with the random Lichtenberg patterns observed in the edge breakdown studies. Both the orientation of these paths and the linear regions of charge depletion shown in the surface voltage measurements (Fig. 9) are along the length of the roll, indicating a preferred direction in the material for electrical conduction. The larger beam voltage (10kV) required for initiating a breakdown on edges parallel to the length of the roll than at right angles further substantiate the assertion that the manufacturing process for forming the sheets could impart a preferred direction in the material, for instance, by aligning the polymer chains of Teflon. Discharges could proceed more readily along the polymer chain because the mobility of electrons along this direction is greater than at right angles across the chain.

Although optical microscopy reveals long straight tracks not present before irradiation, it is not possible to determine if the tracks are on or beneath the surface.

The observed energies of the early electron pulse can be used to provide insight into the discharge and particle emission processes because the time (5ns) for the minimum energy

($\sim$4-5keV) particles to traverse the 9cm distance to the detectors is much less than the duration (600ns) of the particle emissions. This emitted electron energy is composed of two parts; that due to sample surface potential acceleration and that due to J x B forces. The particle emission provides a time history of the breakdown process but only from the instant of onset of the particle emission. For charging potentials of 16-26kV, t is found that emitted particles have energies less than 12keV thereby indicating that the particles are emitted from localized sites whose potentials are substantially less than the breakdown voltage. The presence of electrons having energies in the range of 4-5keV 50ns after the onset of particle emissions indicates that the potential of the emitting site drops to this value very early in this discharge process. Furthermore, the persistence of electrons with this minimum energy for some 600ns would indicate that the potential of the emitting site is maintained at this level. The importance of the surface potential in determining the particle energies is evidenced by the linear relationship between the maximum particle energy and the beam voltage required to initiate breakdown as shown in Figure 17 for shielded edge and exposed edge breakdown studies. The near normal emission of the particles could be indicative of focusing by the electrostatic field.

The early electron pulse accounts for the polarity and the total charge in the return current pulse. The small difference between the charge in the return current and the emitted charge (11 percent) represents the emitted particles that

exited the total charge collector via the beam entrance port.
The total charge in the emitted pulse and in the return current
pulse was found to scale with the area. The area scaling of
the return current pulse observed by others [3, 16] agrees with
the present results.

Attempts to determine the location of the particle emission
site on the sample were inconclusive because the residual charge
after the discharge was not measured.

The pulse of low energy charged particles emitted after
the initial burst of energetic electrons is a quasi-neutral
plasma pulse consisting of approximately equal fluxes of ions
and electrons. The ions are tentatively indentified as singly
ionized carbon by equating the maximum energy measured with the
retarding potential analyzer to the maximum kinetic energy deduced
from the time required by the ions to traverse the sample to
target distance. This is consistent with the observation of
punctures and subsurface cracks and fissures on the samples.
The absence of these plasma emission pulses during most discharge
events, and on all edge breakdowns in particular, provides
additional evidence that multiple discharge processes are opera-
tive. An enumeration of the observed characteristics provides
a means of classifying the processes into two groups with the
duration of the return current pulse a convenient signature.

The return current pulse has been observed to occur as
a short duration pulse ($\sim$20ns) and long duration pulse ($\sim$600ns)
in the present work, but others[3, 16] have reported a longer
pulse duration dependent upon the irradiated area. It has been

found that the short duration return current pulse is always accompanied by the plasma pulse emission. These characteristics have been observed to occur on the initial discharge of samples with shielded edges when a puncture is formed and at times when the threshold voltage reaches local maxima in Figure 6, which could correspond to the formation of new puncture sites. The emission of plasma pulses associated with edge breakdowns has been restricted to studies where the sample edge is at right angles to the preferred axis. In this case, no plasma pulse is observed. The long duration return current pulse is not accompanied by the emission of a plasma pulse. It is observed in shielded edge experiments when the threshold voltage is minimal and in the edge breakdowns studied. The edge breakdowns are always associated with the linear luminous current paths and material damage on the sample. It is interesting to note that the minimum threshold voltages observed on 75μm thick samples with shielded edges and with exposed edges at right angle to the preferred axis are comparable (8-14kV). Although the return current pulse duration is a convenient signature for distinguishing these two classes of discharges, it is the presence of the plasma pulse which provides the insight to differentiate the discharge processes into those where ionization and plasma formation establish the conducting paths and those where other processes such as electron-hole pair formation establish the conducting paths. A classification such as this accounts for linear discharge paths in terms of anisotropic material properties.

The measurements described above provide a basis by which discharge models can be evaluated.[17] The observation of 5-7keV electrons at a time 50ns after initiation of the breakdown indicates that the potential of the emitting site has decreased to values between 5 and 7kV and remains at this level for the duration (600ns) of the particle emission, thereby eliminating phenomenological explanations of breakdown mechanisms having dependence on uniform discharge of the dielectric surface. A discharge model based on a breakdown wave emanating from the breakdown site would incorporate these requirements and account for the dependence of the pulse duration of the return current on the irradiated area.

The near normal emission of particles and presence of particles whose maximum energies are proportional to the breakdown voltage indicate that the electrostatic field is important in focusing and accelerating the emitted particles. The observed emission of ions from the discharge site indicates that plasma effects have to be incorporated into models which describe discharges with short return current pulses. The anisotropic material properties must be incorporated into a model describing breakdowns with linear current paths and long return current pulses. Several models have been proposed to account for the removal of charge from the dielectric surface and for the emission of particles from the surface which incorporate some of these requirements. Inouye and Sellen[8] have suggested that the surface discharge results from a wave that propogates radially from a puncture discharge site whose potential

drops to very small value early in the discharge. This model is consistent with many observations reported herein and can account for the maximum energies and energy spread if the emission takes place in the potential gradient of the discharge wave. The discharge wave in the model is based on a secondary emission mechanism in which the discharge propagates across the dielectric surface. The process is entirely a surface phenomenon and cannot account for the observed anisotropy in the discharge process.

The propagating arc discharge wave suggested by Balmain and Dubois[16] can explain the puncture discharge and associated Lichtenberg patterns. In addition, such a process would produce the plasma emission associated with a puncture breakdown. However, it has been shown that this type of discharge occurs only occasionally.

The cascade ionization wave model described by Beers et al[10] is consistent with the phenomena most often observed. The model is based on avalanche breakdowns within the dielectric material which produce the current carrying paths within the material. Since such a process depends upon the mobility of carriers within the dielectric, any anisoptropy in the carrier mobility would lead to a corresponding anisotropy in the breakdown propagation.

CONCLUSIONS

The results obtained in the course of this work satisfy the primary objectives of the program in providing a physical model for the breakdown and discharge processes taking place on dielectric samples irradiated by a beam of mono-energetic electrons. The threshold voltage measurements, particle emission measurements, and discharge paths studies provide information about the location of the breakdown site, how the surface is discharged, the origin of the return current pulse, and the importance of material properties on the discharge property. These are summarized as follows:

1) The breakdown is initiated at a puncture discharge point for samples with shielded edges and on sample edges for samples with exposed edges.

2) The sample surface is discharged by a breakdown wave expanding from the breakdown site.

3) The accumulated charge is removed by lateral currents flowing at or beneath the sample surface.

4) Anisotropic breakdown properties have been observed which are attributed to differences in electron mobilities along polymer chains and across polymer chains. Alignment of the polymer chains can result from the manufacturing processes for Teflon sheets.

5) The return current is due to the flux of emitted particles (i.e., primary high energy electrons).

6) There appear to be two physically distinct mechanisms whereby the sample is discharged. In one case, ionization and plasma formation are important; in the other, material properties appear to dominate.

7) The duration of the return current pulse appears to be a signature by which these processes in 6) can be identified.

8) The breakdowns lead to material damage that can reduce the efficiency of thermal control surfaces and the ejected effluence can lead to contamination of the spacecraft environment.

These discharge characteristics can be used as a criteria for evaluating mathematical models and as a guide for spacecraft engineers. Of particular significance to the engineers is the possible influence of material anisotropy on the dielectric area that can be discharged in a given event.

A number of significant questions about certain features of this discharge process remain unanswered. These include the location of the particle emission site, the reason why the return current pulse duration is shorter when the plasma pulse is present than it is without the plasma pulse, and the exact nature of the electrical path when ionization and material damage are not dominant. A measurement of these properties together with the expansion velocity of the surface breakdown wave are the topics of future studies to provide a more quantitative evaluation of discharge models.

SUMMARY

Under NASA Research Grant No. NSG-3145 entitled, "Laboratory Simulation of Irradiation-Induced Dielectric Breakdown in Spacecraft Charging," Colorado State University had undertaken a theoretical and experimental investigation of the phenomenon of spacecraft charging with the following program goals: development of spacecraft charging laboratory simulator, study of electrical discharge characteristics of irradiated dielectric samples, identification of electrical breakdown paths over surfaces and within the dielectric material, correlation of electrical discharge sites with pre-existing material defects, determination of the origin and destination of particles emitted from the electrical discharges, and evaluation of the role of charge and energy balance in the modeling of the discharge phenomena. This program was transferred to the Research and Development Center, Inland Motor Divisions, Kollmorgen Corporation in June of 1979.

The characteristics of electrical discharges on silverbacked Teflon samples irradiated by a beam of energetic electron (0-34keV) were studied using Faraday cups, retarding potential analyzers, photomultipliers, surface voltage probes and transient current probes. The dependence of the threshold voltage on sample thickness, condition of edges, and material properties was studied. Angular distribution and energy distribution of emitted particles were measured with retarding potential analyzers. The luminous discharge patterns were compared with optical and scanning electron micrographs of material damage. The dependence of total charge in emitted particles and return current pulses was measured as was the surface potential profile before and after electrical breakdown. The results indicate that the dielectric breakdown is initiated at puncture discharge sites or sample edges and the sample surface is discharged by a breakdown wave propagating from the breakdown site with the accumulated charge being removed by lateral currents flowing on or beneath the dielectric surface. The dielectric appears to be discharged by two different processes: a plasma-dominated ionization mode with substantial material damage and a material-propertydominated mode with substantial anisotropy. The duration of the return current pulse is a convenient signature for identifying these modes. A pulse of energetic electrons accounts for the return current pulse.

The results obtained are of interest to the spacecraft engineer for two reasons. First of all, the measurements provide a physical picture of the discharge processes which can be used to evaluate predictive models for the discharge process. Secondly, the material anisotropy observed in Teflon

SUMMARY (Continued)

can substantially affect the charged area that can be dis-
charged. Furthermore, the results indicate a number of
future measurements that should be made for a more quanti-
tative evaluation of discharge models. These include the
determination of the emission site location, the propagation
velocity of the discharge wave with respect to the material
anisotropy of Teflon, the reason why a short duration return
current pulse results whenever ionization and plasma effects
are important and the nature of the processes whereby an
electrical path is established when ionization and vapori-
zation are not the dominant processes.

ACKNOWLEDGMENTS

REFERENCES

[1] Spacecraft Charging Technology, NASA Conference Publication 2071, AFGL-TR-79-0082, 1978.

[2] A. Rosen, "Spacecraft Charging: Environment Induced Anomalies," AIAA Paper, AIAA 13th Aerospace Science Meeting, Pasadena, CA., 75-91, 1975.

[3] P. R. Aron and J. V. Staskus, "Area Scaling Investigations of Charging Phenomena," Spacecraft Charging Technology, NASA Conference Publication 2071, AFGL-TR-79-0082, 485-506, 1978.

[4] K. G. Balmain, "Scaling Law and Edge Effects for Polymer Surface Discharges," Spacecraft Charging Technology, NASA Conference Publication 2071, AFGL-TR-79-0082, 646-656, 1978.

[5] N. J. Stevens, C. K. Purvis and J. V. Staskus, "Insulator Edge Voltage Gradient Effects in Spacecraft Charging Phenomena," IEEE Transactions on Nuclear Science, v NS-25, n6, 1304-1312, Dec., 1978.

[6] F. D. Berkopec, N. J. Stevens and J. C. Sturman, "The Lewis Research Center Geomagnetic Substorm Simulation Facility," Proceedings of the Spacecraft Charging Technology Conference, Air Force Survey in Geophysics, No. 364, AFGL-TR-0051, NASA TMX-73537, C. P. Pike and R. R. Lovell, ed., 423-430, 1977.

[7] T. M. Flanagan, R. Denson, C. E. Mallon, M. J. Treadway and E. P. Wenaas, "Effect on Laboratory Simulation Parameters on Spacecraft Dielectric Discharges," IEEE Trans. Nucl. Sci., NS-26, 5134 (1979).

[8] G. T. Inouye and J. M. Sellen, Jr., "A Proposed Mechanism for the Initiation and Propagation of Dielectric Surface Discharges," Proceedings of the 1978 Symposium on the Effects of the Ionosphere on Space and Terrestrial Systems, 1-4, 1978.

[9] R. Leadon and J. Wilkenfeld, "Model for Breakdown Process in Dielectric Discharges," Spacecraft Charging Technology, NASA Conference Publication 2071, AFGL-TR-79-0082, 704-710, 1978.

[10] B. L. Beers, V. W. Pine, H. C. Hwang, and H. W. Bloomberg, "Negative Streamer Development in FEB Teflon," IEEE Trans. Nucl. Sci., NS-26, 5127 (1979).

REFERENCES (Continued)

[11] E. J. Yadlowsky, R. C. Hazelton and R. J. Churchill, "Characterization of Electrical Discharges on Teflon Dielectrics Used as Spacecraft Thermal Control Surfaces," Spacecraft Charging Technology, NASA Conference Publication 2071, AFGL-TR-79-0082, 632-645, 1978.

[12] E. J. Yadlowsky, R. C. Hazelton and R. J. Churchill, "Puncture Discharges in Surface Dielectrics as Contaminant Sources in Spacecraft Environments," Proceedings of the USAF/NASA International Spacecraft Contamination Conference, AFML-TR-78-190, NASA-CP-2039, J. M. Jemola, ed., 945 (1978).

[13] DuPont Bulletin T-4D, "Electrical Properties of Teflon FEP Fluoro Carbon Film."

[14] N. J. Stevens, F. D. Berkopec, J. V. Staskus, R. A. Blech and S. J. Narciso, "Testing of Typical Spacecraft Materials in a Simulated Substorm Environment," Proceedings of the 1976 Spacecraft Charging Technology Conference, C. P. Pike and R. R. Lovell, eds., Report AFGL-TR-0051/NASA TMX-73537, 431 (1977).

[15] L. B. Fogdall, S. S. Cannaday, M. C. Wilkinson, E. R. Crutcher, III, and P. S. P. Wei, "Combined Environmental Effects on Polymers," Report on Work Performed on Contract NAS1-13530, NASA-Langley Research Center and Contract CSC-IS-556, Communications Satellite Corp.

[16] K. G. Balmain and G. R. Dubois, "Surface Discharges on Teflon, Mylar and Kapton," IEEE Trans. Nucl. Sci. NS-26, 5146 (1979).

[17] R. C. Hazelton, R. J. Churchill and E. J. Yadlowsky, "Measurements of Particle Emission from Discharge Sites in Teflon Irradiated by High Energy Electron Beams," IEEE Trans. Nucl. Sci., NS-26, 5141 (1979).